

1 **Supplementary materials**

2 **Supplementary methods**

3 **Flow cytometric analysis of neutrophils. *Neutrophils Heart infiltrates.*** PBS perfused hearts
4 were disaggregated using the Gentle MACs disaggregator (Miltenyi Biotec) and cells were stained
5 with the following antibodies: CD45-V450, Ly6G APC-Cy7, B220 PE-Cy7, CD3 APC, CD4 PE, CD8
6 PerCP-Cy5.5, F4/80 FITC. Neutrophils were identified as CD45+Ly6G+ cells. ***Circulating and***
7 ***splenic neutrophils.*** Circulating and splenic neutrophils were identified in freshly collected blood
8 and spleen by flow cytometry as CD45 positive cells and CD45/Ly6G double positive cells. ¹

9 **Heart Proteomic analysis by nanoLC/MS-MS.** Four hearts of mice with sickle cell disease (HbS,
10 SS) and four wt controls were lysed as previously reported.^{2,3} The tryptic peptide mixtures, ob-
11 tained by shotgun procedure onto S-trap cartridge,⁴ were analyzed in duplicate by nanoLC-MS/MS
12 using a Q-Exactive mass spectrometer (Thermo Scientific, Bremen, Germany) equipped with a
13 nano-electrospray ion source (Proxeon Biosystems) and a nanoUPLC Easy nLC 1000 (Proxeon
14 Biosystems). Peptide separations occurred on a homemade reverse phase silica capillary column
15 (75 μ m i.d., 15 cm long), packed with 1.9- μ m ReproSil-Pur 120 C18-AQ (Dr. Maisch GmbH, Ger-
16 many). A gradient of eluents A (distilled water with 0.1% v/v formic acid) and B (acetonitrile with
17 0.1% v/v formic acid) was used for chromatographic separation (300 nL/min flow rate), from 2% B
18 to 40% B in 88 minutes. Full scan spectra were acquired with the lock-mass option, resolution set
19 to 70,000 and mass range from m/z 300 to 2000 Da. The ten most intense doubly and triply
20 charged ions were selected and fragmented (NCE= 27). Raw data were analyzed with MaxQuant
21 1.5.2.8 for protein identification and quantification as reported in Andolfo et al.⁵, using Mus muscu-
22 lus (revised 2021) as database. Statistical analysis was performed by Perseus software (Perseus
23 version 1.6.15.0).⁶ For the statistical analysis, a student's t-test was applied with a p-value cut-off
24 of 0.05 and with a $|\log_2FC|$ cut-off of 0.5. ⁷

25 **Immunoblot analysis.** Frozen heart from each studied group were homogenized and lysed with
26 iced lyses buffer (150 mM NaCl, 25 mM bicine, 0.1% SDS, 2% Triton X-100, 1 mM EDTA, protease
27 inhibitor cocktail tablets (Roche), 1 mM Na3VO4 final concentration) then centrifuged 30 min at
28 4°C at 12,000 g.^{3,8} Specific antibodies used are: anti Nrf2-phospho-S40 (Clone EP1809Y, dilution
29 1:1000, 75 μ gr/ul loaded, AbCam, Cambridge, UK); anti-Nrf2 (dilution 1:1000, 75 μ gr/ul loaded,
30 AbCam, Cambridge, UK); anti Phospho (Tyr653/654) FGF Receptor1 (FGF Rec) (dilution 1:1000,
31 75 μ gr/ul loaded) from GeneTex, Inc; anti FGF Receptor (FGF Rec) (dilution 1:1000, 75 μ gr/ul
32 loaded) from GeneTex, Inc FGF; anti Phospho (Tyr740) PDGF Receptor (PDGF Rec) (dilution
33 1:1000, 75 μ gr/ul loaded) from GeneTex, Inc; anti PDGF Receptor (PDGF Rec) (dilution 1:1000, 75
34 μ gr/ul loaded) from GeneTex, Inc; anti Phospho-Tyrosine (clone PY99 from SCBT, Santa Cruz, CA

(dilution 1:3000, 75 µgr/ul loaded) and clone 4G10 from Merck KGaA, Darmstadt, Germany (dilution 1:1600, 75µgr/ul loaded); anti Phospho (Ser536) NF-kB p65 (dilution 1:1000, 75 µgr/ul loaded) and anti NF-kB p65 (clone C22B4) (dilution 1:1000, 75 µgr/ul loaded) from Cell Signaling Technology (Danvers, MA, USA); anti VCAM-1 (R and D Systems, Minneapolis, MN, USA (dilution 1:1000, 40 µgr/ul loaded); P-Selectin (clone AK4, dilution 1:1000, 50 µgr/ul loaded) form AbCam, Cambridge, UK; anti Endothelin-1 (ET-1) form AbCam, Cambridge, UK (dilution 1:1000, 75 µgr/ul loaded); anti TBXS (dilution 1:1000, 75 µgr/ul loaded; Cayman, Ann Arbor, MI, USA); anti NLRP3 (dilution 1:1000, 75 µgr/ul loaded) form Adipogen AG, Fuellinsdorf, Switzerland; anti-heme oxygenase 1(HO-1) form SCBT (Santa Cruz, CA, USA (dilution 1:1000, 50 µgr/ul loaded); anti Nqo1 from Santa Cruz Biotechnology, Inc, CA, USA (clone C-19; dilution 1:1000, 75 µgr/ul loaded); anti Peroxiredoxin 2 (Prx2; kindly provided by Prof. Ho Zoo Chae, School of Biological Science and Technology, Chonnam National University, Gwangju, Korea (dilution 1:2000, 20 µgr/ul loaded)); anti Peroxiredoxin 3 (Prx3) form AbCam, Cambridge, UK (dilution 1:1000, 75 µgr/ul loaded); anti P-Smad 2 form ABclonal Inc, Woburn, MA, USA (dilution 1:1000, 75 µgr/ul loaded); anti Smad2 form ABclonal Inc, Woburn, MA, USA (dilution 1:1000, 75 µgr/ul loaded); anti P-Smad 3 form ABclonal Inc, Woburn, MA, USA (dilution 1:1000, 75 µgr/ul loaded); anti Smad 3 form ABclonal Inc, Woburn, MA, USA (dilution 1:1000, 75 µgr/ul loaded); anti Smad 4 form ABclonal Inc, Woburn, MA, USA (dilution 1:1000, 75 µgr/ul loaded); anti Smad 7 form ABclonal Inc, Woburn, MA, USA (dilution 1:1000, 75 µgr/ul loaded); anti HIF 1 α (clone H-206, Santa Cruz Biotechnology Inc, CA, USA (dilution 1:1000, 50 µgr loaded)); anti HIF 2 (EPAS-1, clone 190b, Santa Cruz Biotechnology Inc, CA, USA (dilution 1:1000, 75 µgr loaded)); anti Phospho (Tyr1175) VEGF Receptor (Rec) (clone 19A10, dilution 1:1000, 75 µgr loaded) from Cell Signaling Technology (Danvers, MA, USA); anti VEGF Receptor (Rec) (clone 55B11, dilution 1:1000, 75 µgr loaded) from Cell Signaling Technology (Danvers, MA, USA); anti VEGF form AbCam, Cambridge, UK (dilution 1:1000, 75 µgr/ul loaded); anti Angiopoietin 1 (Ang 1) form AbCam, Cambridge, UK (dilution 1:1000, 75 µgr/ul loaded); anti Angiopoietin 2 (Ang 2) form AbCam, Cambridge, UK (dilution 1:1000, 75 µgr/ul loaded); anti ATF6 from Novus Biologicals Europe, Abingdon, UK (clone 70B1413.1, dilution 1:1000, 75 µgr/ul loaded); anti GADD34 form AbCam, Cambridge, UK (dilution 1:1000, 75 µgr/ul loaded); anti ATF 4 (clone D4B8; dilution 1:1000, 75 µgr/ul loaded) from Cell Signaling Technology (Danvers, MA, USA); anti CHOP from Invitrogen (Thermo Fisher Scientific Inc) (clone 9C8, dilution 1:1000, 75 µgr/ul loaded); anti Caspase 1 form AbCam, Cambridge, UK (dilution 1:1000, 75 µgr/ul loaded); anti pro Caspase 3 form AbCam, Cambridge, UK (clone E83-103; dilution 1:1000, 75 µgr/ul loaded); anti ICAM-1 (clone EP1442Y, dilution 1:1000, 75 µgr/ul loaded, AbCam, Cambridge, UK); anti Gpx 1 (dilution 1:1000, 50 µgr/ul loaded, clone N-20, Santa Cruz Biotechnology, CA, USA); anti ANP (dilution 1:500, 75 µgr/ul loaded; Gene Tex, Irvine, CA, USA) and anti GAPDH from SCBT (Santa Cruz, CA, USA (dilution 1:5000, 50 µgr/ul loaded)). Secondary donkey anti-rabbit IgG (dilution 1:10000) and anti-mouse IgG (dilution 1:5000) HRP conjugated were from GE

Healthcare Life Sciences (Little Chalfont, UK); secondary donkey anti goat IgG (dilution 1:10000) HRP conjugated was from SCBT, secondary donkey anti rat IgG (dilution 1:5000) HRP conjugated was from AbCam. Blots were developed with Luminata Forte Chemiluminescent HRP Substrate from Merk Millipore (Burlington, MA, USA), and images were acquired with the Alliance Q9 Advanced imaging system (Uvitec, UK). Densitometric analyses were performed with the Nine Alliance software (Uvitec, UK). Immunoprecipitations (IP) assays of anti-phospho-Tyr proteins from heart lysate were carried out using the Protein A Agarose (Thermo Fisher scientific, USA) and the mix of the anti phospho-Tyrosine monoclonal antibodies PY99 (Santa Cruz Biotechnology, USA) and 4G10 (Merck Group, De). Oxidized proteins were monitored by using the Oxyblot Protein Oxidation Detection Kit (EMD Millipore) following the manufacturer instructions (6) (8).

Heart molecular analysis. For nucleic acid extraction, hearts snap frozen in liquid nitrogen following excision were homogenized in RNA lysis buffer (Zymo Research) using the GentleMACStissue dissociator (Miltentyi Biotec), and clear lysates were loaded onto silica spin columns for RNA/miRNA purification following the manufacturer's protocol. The extracted nucleic acids were quantified using a UV nanophotometer, reverse transcribed, and used in quantitative PCR analyses using mRNA or miRNA assays, or preloaded array plates (miRCURY LNA miRNA Focus PCR Panel Cardiovascular Disease). All reagents for reverse transcription, primers, and master mixes for PCR were from Qiagen. Expression of miRNAs was determined with quantitative PCR and normalized using RNU5G and RNU1A1 as housekeepers. For RT-PCR analysis data were expressed as normalized levels using GAPDH as reference gene. The following primers were used: GAPDH (forward: CATCACTGCCACCCAGAAGACTG; reverse: ATGCCAGTGAGCTTCCCGTTTCAG) FN1 (forward: GCCAGGAACCGAGTACACC; reverse: CAGTTGGGGAAGCTCATCTGT), IL1b (forward: GCCACCTTTTGACAGTGATGAG; reverse: GACAGCCCAGGTCAAAGGTT), IL18 (forward: TACAAGCATCCAGGCACAGC; reverse: CAGGCAGGAGTCCAGAAAGC)

Echocardiography. Transthoracic echocardiography was performed with a Vevo 2100 echocardiograph (Visual Sonics, Toronto, Canada) equipped with a 22-55 MHz transducer (MicroScan Transducers, MS500D) as previously described.⁹ Echocardiographic parameters were measured at the level of the papillary muscles in the parasternal short-axis view (M mode). Fractional shortening (FS) was calculated as previously described.¹⁰ Diastolic parameters were measured with tissue Doppler and pulsed wave Doppler techniques in the apical long-axis view as reported in Schnelle M et al. 2018.⁹ Cardiac function was assessed when heart rate was 400-450 bpm.

Heart histological analysis. Paraffin-embedded tissue blocks were stained with: hematoxylin and eosin (H&E) for assessment of cardiomyocyte area, PicroSirius red for fibrosis evaluation and Perls' staining for iron content detection. Cardiomyocyte area and fibrosis were quantified as described previously.¹¹ Tissues were fixed in 10% neutral buffered formalin and embedded in paraffin. After the embedding, 3 µm-thick sections were cut and stained with hematoxylin and eosin (Bio-

Optica, Italy) for histological examination. For immunohistochemical analysis, after the appropriate antigen retrieval procedure, slides were incubated with the following primary antibodies: rabbit anti-mouse LY6G antibody (#87048, Cell Signaling), rabbit anti-mouse activated caspase-3 antibody (AF835, R&D), mouse anti-mouse α -smooth muscle actin (A5228, clone 1A4, Sigma-Aldrich), followed by the appropriate secondary antibody (Envision rabbit, Dako). For α -smooth muscle actin, endogenous mouse Ig staining was reduced by using M.O.M.[®] (Mouse on Mouse) ImmPRESS[®] HRP (Peroxidase) Polymer Kit (MP-2400) (Vector Laboratories, Newark, USA) according to manufacturer's instructions. Immunostainings were developed with DAB Chromogen system (Dako). The whole slides were scanned with Nanozoomer scanner (Hamamatsu) and analyzed with NDP.view2 software by counting the number of positive brown cells and the total heart area. For immunofluorescence analysis, slides were incubated with rabbit anti-mouse LY6G antibody (#87048, Cell Signaling), rabbit anti-CD206 (#24595, Cell Signaling), rabbit anti-CD31 (ab182981, Abcam), rabbit anti-VEGFR (#9698, Cell Signaling), mouse monoclonal anti-Gal-3 (ab2785, Abcam). Secondary antibodies used were goat anti-rabbit Alexa Fluor 488 (A11008) or goat anti-mouse Alexa Fluor 546 (A11030) both from ThermoFisher. Immunostainings were developed using TSA Plus Cyanine 3 (NEL744001KT, Akoya Biosciences) Nuclei were stained with Dapi (Sigma), and images were acquired by Zeiss LSM800 confocal microscope. Perls and collagen staining as well as cardiomyocyte areas were carried out on hearts from healthy and SS mice. Details are reported in Supplementary data.

ELISA assays. Plasma pro-BNP was measured by NT-pro-BNP ELISA kit (Nordic BioSite AB, Sweden). Serum Galectin-3 (Gal-3) and pro-collagen C-proteinase enhancer-1 (Pcpe-1) were determined by ELISA according to manufacturer's instruction (Galectin-3: ab203369, Abcam, Cambridge, UK; Pcpe-1: MBS724700, MyBioSource Inc., San Diego, CA 92195-3308, USA)

Statistics. Two tailed unpaired Student t-test or two-way analysis of variance with Tukey's multiple comparisons were used for data analyses. Whenever indicated we used unpaired Student t-test or one-way ANOVA algorithm for repeated measures using Graph-pad 10.2. Normality was assessed with Shapiro-Wilk test. Data show values from individual mice and are presented with mean \pm SEM. Differences with $p < 0.05$ were considered significant.

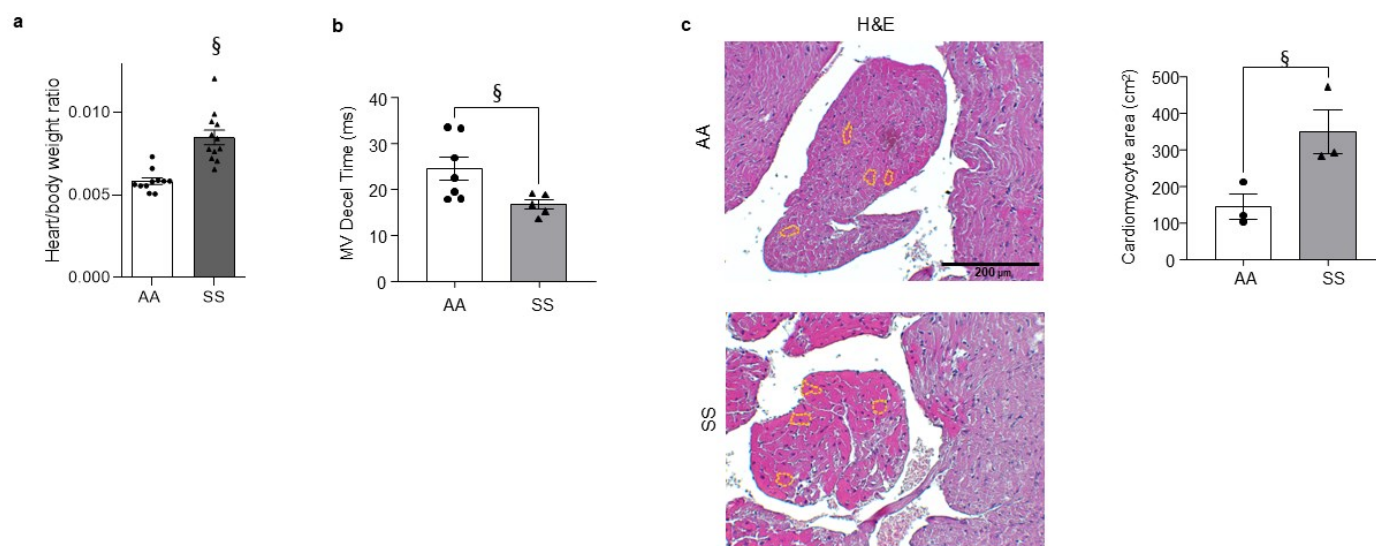
Supplementary references

1. Federti E, Matte A, Recchiuti A, et al. In Humanized Sick Cell Mice, Imatinib Protects Against Sick Cell-Related Injury. *Hemasphere*. 2023;7(3):e848.
2. Federti E, Matte A, Ghigo A, et al. Peroxiredoxin-2 Plays a Pivotal Role as Multimodal Cytoprotector in the Early Phase of Pulmonary Hypertension. *Free Radic Biol Med*. 2017.
3. Federti E, Vinchi F, Iatcenko I, et al. Duality of Nrf2 in iron-overload cardiomyopathy. *Haematologica*. 2023;108(5):1335-1348.

- 143 4. Palinski W, Monti M, Camerlingo R, et al. Lysosome purinergic receptor P2X4 regulates
144 neoangiogenesis induced by microvesicles from sarcoma patients. *Cell Death Dis.* 2021;12(9):797.
- 145 5. Andolfo I, Monaco V, Cozzolino F, et al. Proteome alterations in erythrocytes with PIEZO1 gain-of-
146 function mutations. *Blood Adv.* 2023;7(12):2681-2693.
- 147 6. Tyanova S, Temu T, Sinitcyn P, et al. The Perseus computational platform for comprehensive analysis
148 of (prote)omics data. *Nat Methods.* 2016;13(9):731-740.
- 149 7. Iacobucci I, Monaco V, Cane L, et al. Spike S1 domain interactome in non-pulmonary systems: A role
150 beyond the receptor recognition. *Front Mol Biosci.* 2022;9:975570.
- 151 8. Matte A, Recchiuti A, Federti E, et al. Resolution of sickle cell disease-associated inflammation and
152 tissue damage with 17R-resolvin D1. *Blood.* 2019;133(3):252-265.
- 153 9. Schnelle M, Catibog N, Zhang M, et al. Echocardiographic evaluation of diastolic function in mouse
154 models of heart disease. *J Mol Cell Cardiol.* 2018;114:20-28.
- 155 10. Perino A, Ghigo A, Ferrero E, et al. Integrating cardiac PIP3 and cAMP signaling through a PKA
156 anchoring function of p110gamma. *Mol Cell.* 2011;42(1):84-95.
- 157 11. Li M, Sala V, De Santis MC, et al. Phosphoinositide 3-Kinase Gamma Inhibition Protects From
158 Anthracycline Cardiotoxicity and Reduces Tumor Growth. *Circulation.* 2018;138(7):696-711.

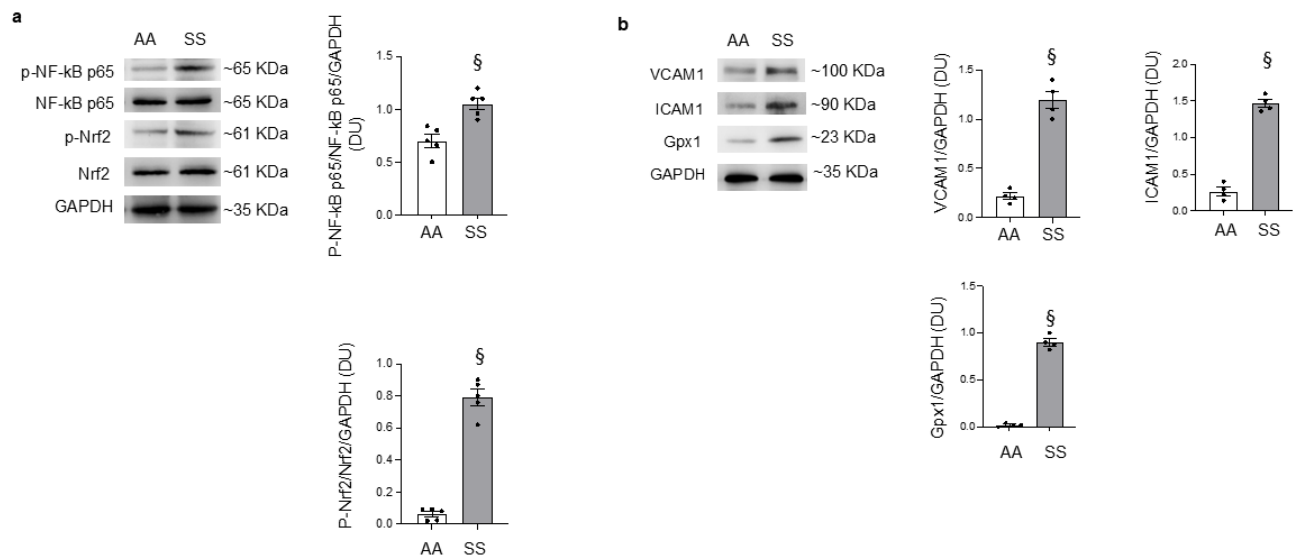
159 **Supplementary Figures**

Figure 1S



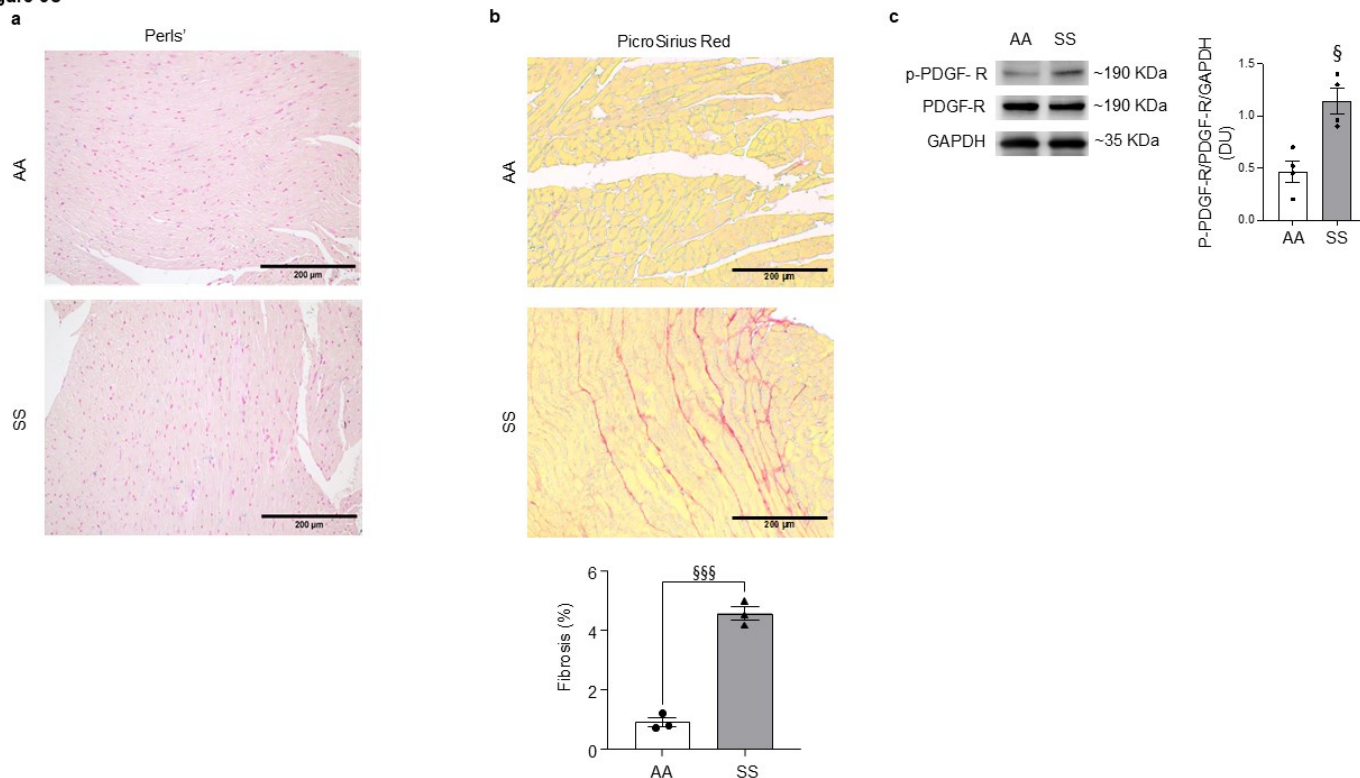
160 **Figure 1S. a)** Heart weight to mouse weight ratio in healthy AA mice and sickle cell (SS) mice.
161 Data are presented as means \pm SEM (n=11-12), § p <0.05 compared to AA normoxia by t-test. **b)**
162 Diastolic function (measured as mitral valve deceleration time, MV decel time) in AA and SS mice.
163 Data are presented as means \pm SEM (n= 5-7) *p<0.05 by t-test. **c)** Representative images of he-
164 matoxylin & eosin (H7E) staining and relative quantification of cardiomyocyte area in heart sec-
165 tions from AA and SS mice. Representative cardiomyocyte areas are shown by dashed lines. Data
166 are presented as means \pm SEM (n= 3) *p<0.05, by t-test.

Figure 2S



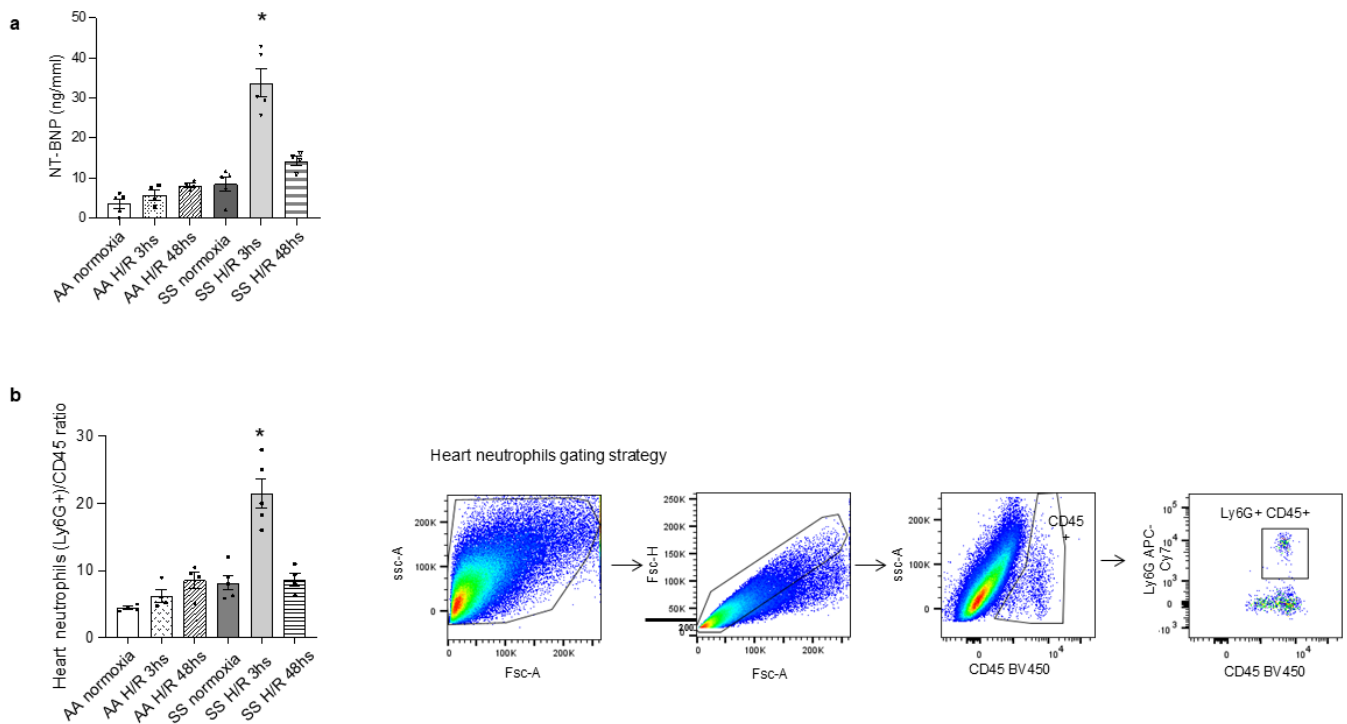
167 **Figure 2S. a)** Immunoblot analysis, using specific antibodies against phosphorylated (p-)NF-κB
168 p65, NF-κB p65, p- Nrf2 and Nrf2 in heart from healthy (AA) and sickle cell (SS) mice. 75 µg/µL of
169 protein loaded on an 11% T, 2.5%C polyacrylamide gel. GAPDH serves as protein loading control.
170 One representative gel from 5 with similar results is shown. Densitometric analysis of immunoblots
171 is shown on the right. Data are presented as means ±SEM (n=5), § p<0.05 compared to AA
172 normoxia by t-test. **b)** Immunoblot analysis using specific antibodies against VCAM-1, ICAM1,
173 GPX 1 in heart from healthy (AA) and sickle cell (SS) mice. 75 µg/µL of protein loaded on an 11%
174 T, 2.5%C polyacrylamide gel. GAPDH serves as protein loading control. One representative gel
175 from 4 with similar results is shown. Densitometric analysis of immunoblots is shown on the right.
176 Data are presented as means ±SEM (n=5), § p<0.05 compared to AA normoxia by t-test.

Figure 3S



177 **Figure 3S. a)** Representative heart sections from AA and SS mice stained with Perls' reaction. **b)**
 178 Representative images of PicroSirius Red staining and relative quantification in heart sections from
 179 healthy (AA) and sickle cell (SS) mice. Data are presented as means \pm SEM (n=3), §§§ p<0.02
 180 compared to AA by t-test. **c)** Immunoblot analysis using specific antibodies against phosphorylated
 181 (p-) PDGF R and PDGF R (**left panel**) in heart from healthy (AA) and SS mice. One representative
 182 gel from 4 gels with similar results is shown. 75 μ g/ μ L of protein loaded on an 11% T, 2.5%C poly-
 183 acrylamide gel. GAPDH serves as protein loading control. Densitometric analysis immunoblots are
 184 shown in the right panel. Data are presented as means \pm SEM (n= 4), § p<0.05 compared to AA
 185 normoxia by t-test.

Figure 4S



186 **Figure 4S. a)** Plasmatic NT-pro-BNP level in of healthy (AA) and sickle (SS) mice in normoxia (N)
 187 and exposed to H/R: hypoxia (8% oxygen; 10 hours), followed by reoxygenation (21% oxygen; 3
 188 hours or 48 hours). Data are presented as mean \pm SEM (n = 4-9); *p<0.05 compared to normoxia
 189 by t-test. **b)** Heart neutrophils infiltration identified by flow cytometric analysis as CD45+Ly6G+
 190 cells in AA and SS mice treated as in a. Data are presented as mean \pm SEM (n = 4-5) *p<0.05
 191 compared to normoxia by t-test. Heart neutrophils infiltrate gating strategy (**right panel**).

Figure 5S

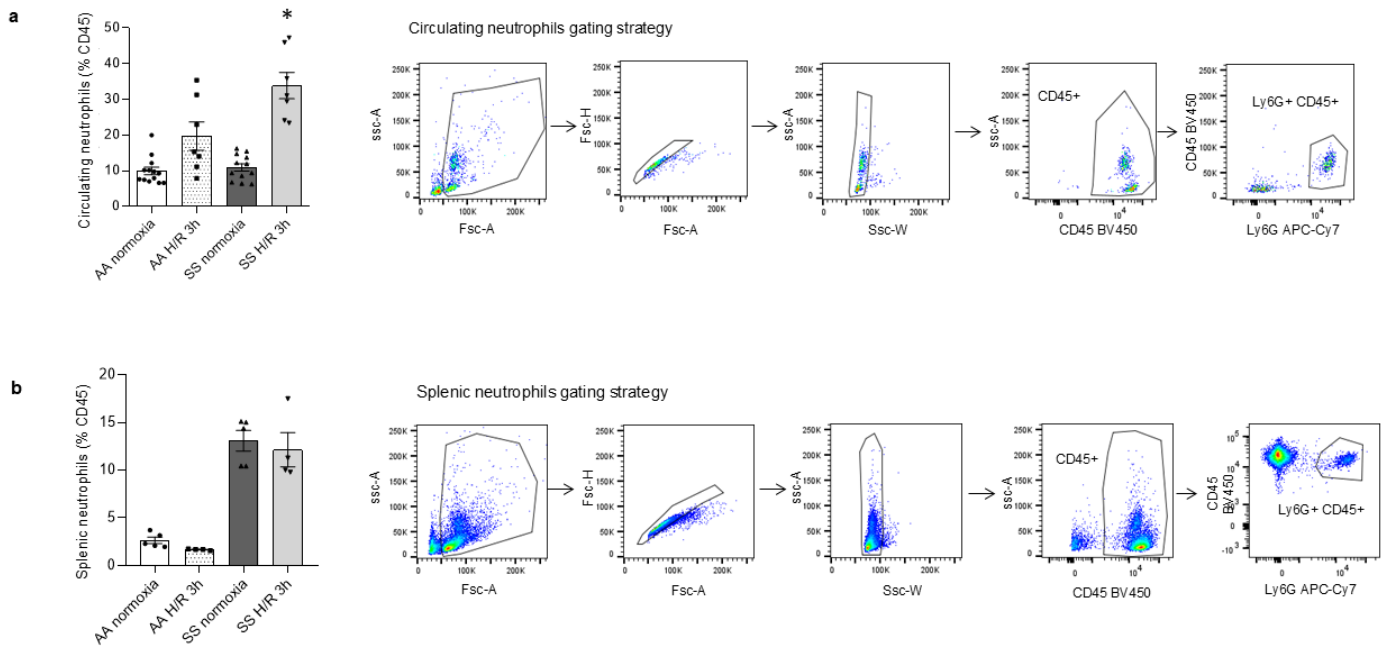
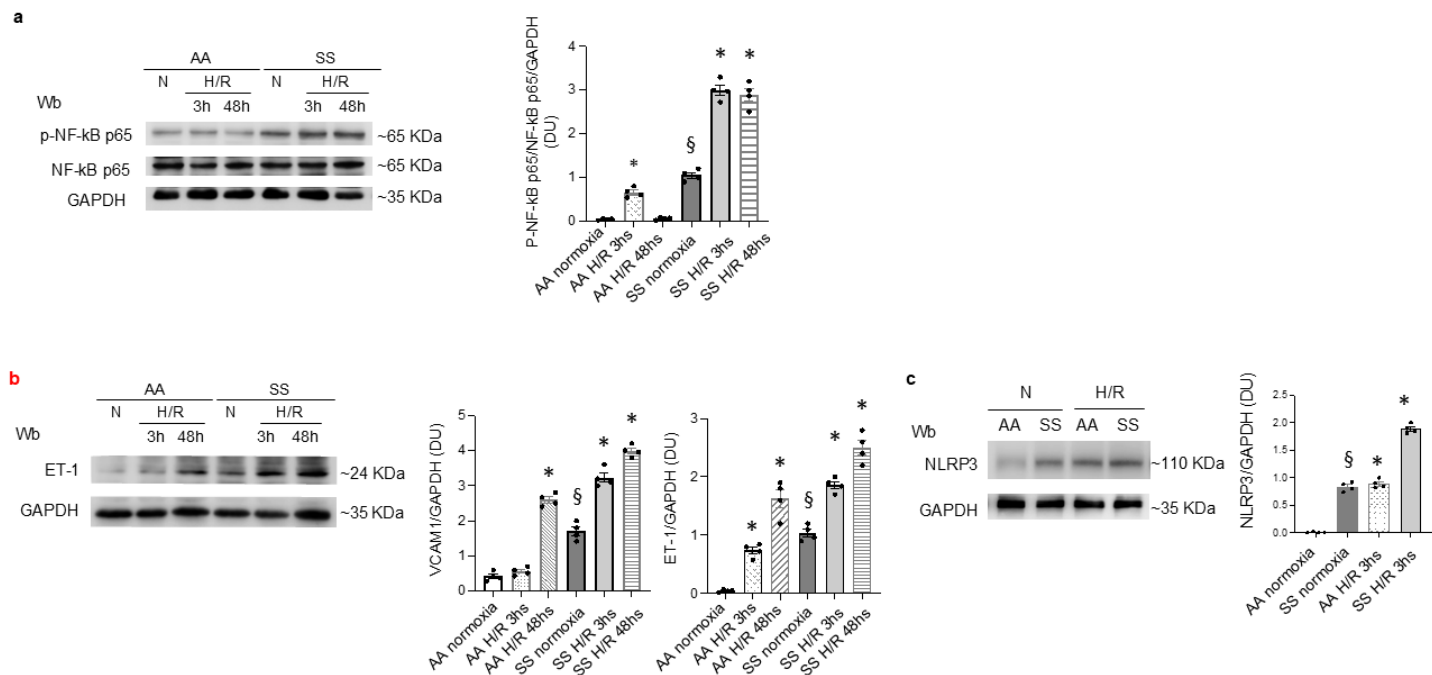


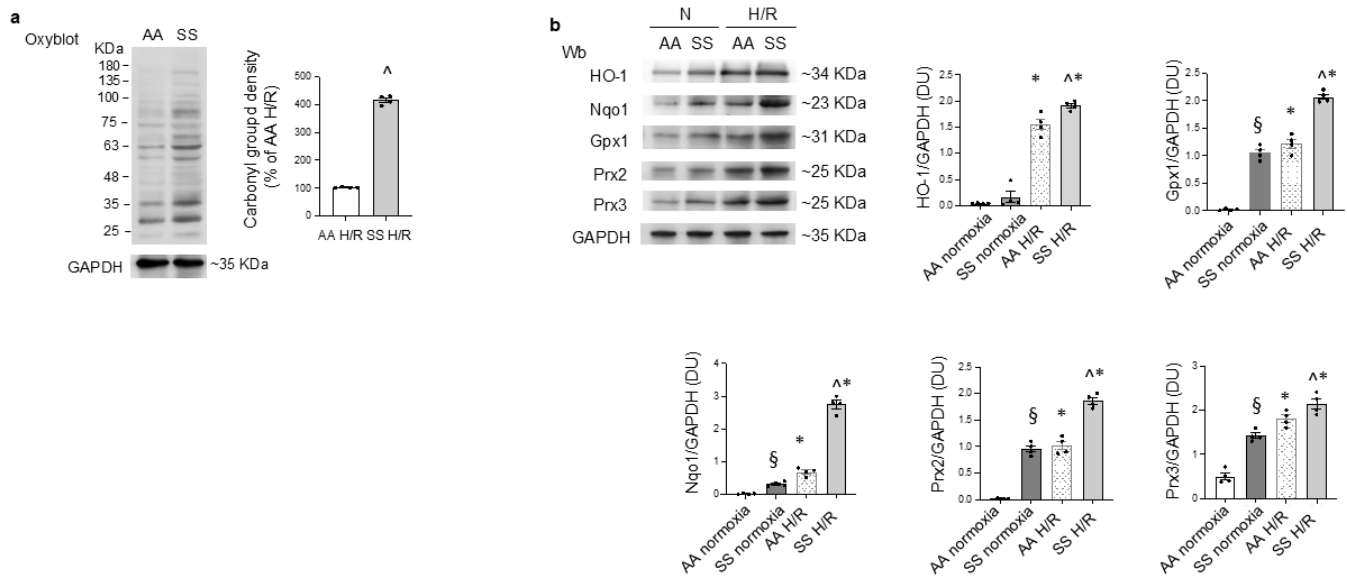
Figure 5S. a) Circulating neutrophils as CD45+Ly6G+ cells in healthy (AA) and sickle cell (SS) mice under normoxia (N) and exposed to H/R: hypoxia (8% oxygen; 10 hours), followed by reoxygenation (21% oxygen; 3 hours). Data are presented as means \pm SEM (n= 7-13), *p<0.05 compared to normoxia by t-test. **Right panel.** Gating strategy. **b)** Splenic neutrophils as CD45+Ly6G+ cells as in (a). Data are presented as means \pm SEM (n= 4-5).

Figure 6S



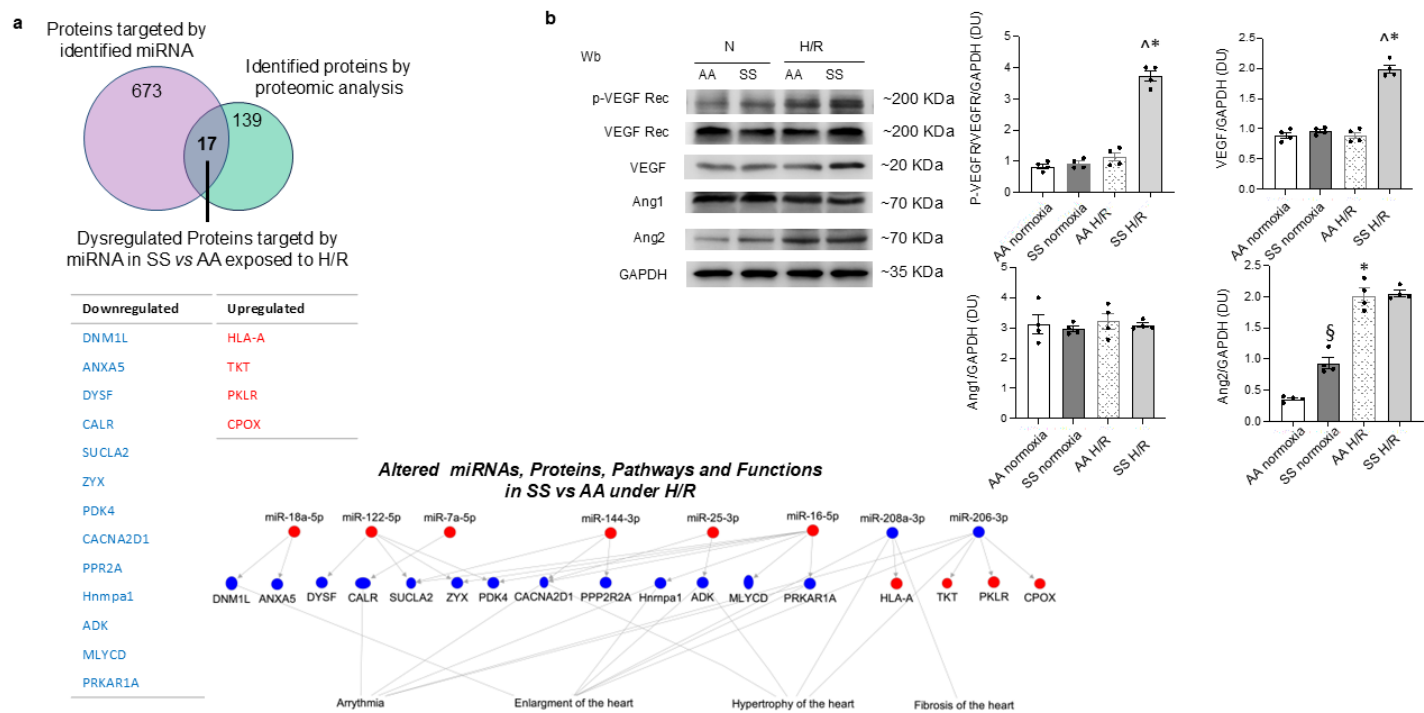
197 **Figure 6S. a)** Immunoblot analysis, using specific antibodies against phosphorylated (p-)NF-κB
198 p65 and NF-κB p65 in heart from healthy (AA) and sickle cell (SS) mice under normoxia (N) and
199 exposed to H/R: hypoxia (8% oxygen; 10 hours), followed by reoxygenation (21% oxygen; 3 hours
200 or 48 hours). 75 µg/µL of protein loaded on an 11% T, 2.5%C polyacrylamide gel. GAPDH serves
201 as protein loading control. One representative gel from 4 with similar results is shown. Densitomet-
202 ric analysis of immunoblots is shown in the right panel. Data are presented as means ±SEM (n=4),
203 *p<0.05 compared to normoxia; § p<0.05 compared to AA normoxia by one-way ANOVA. **b)** Im-
204 munoblot analysis, using specific antibodies against ET-1 in heart from healthy (AA) and sickle cell
205 SS mice under normoxia (N) and exposed to H/R: hypoxia (8% oxygen; 10 hours), followed by re-
206 oxygenation (21% oxygen; 3 hours or 48 hours). 50 µg/µL of protein loaded on an 11% T, 2.5%C
207 polyacrylamide gel. GAPDH serves as protein loading control. One representative gel from 4 with
208 similar results is shown. Densitometric analysis of immunoblots is shown on the right. *p<0.05
209 compared to normoxia; § p<0.05 compared to AA normoxia by one-way ANOVA ^p<0.05
210 compared to AA H/R at 48 hours. **c)** Immunoblot analysis using specific antibodies against NLRP3
211 in heart from healthy (AA) and sickle cell (SS) mice as in (a). 75 µg/µL of protein loaded on an 8%
212 T, 2.5%C polyacrylamide gel. GAPDH serves as protein loading control. One representative gel
213 from 4 with similar results is shown. Densitometric analysis of immunoblots is shown on the right.
214 Data are presented as means ±SEM (n=4), *p<0.05 compared to normoxia; § p<0.05 compared to
215 AA normoxia by one-way ANOVA.

Figure 7S



216 **Figure 7S. a)** OxyBlot analysis of the soluble fractions of heart from healthy (AA) and sickle cell
217 (SS) mice exposed to H/R: hypoxia (8% oxygen; 10 hours), followed by reoxygenation (21% oxy-
218 gen for 3 hours). The carbonylated proteins (1 mg) were detected by treating with 2,4-dinitro-
219 phenylhydrazine and blotted with anti-DNP antibody. GAPDH serves as protein loading control.
220 Quantification of band area is shown in right panel. Data are presented as means \pm SEM (n=4),
221 ^p<0.05 compared to AA mice exposed to H/R by t-test. **b)** Immunoblot analysis, using specific an-
222 tibodies against HO-1, Gpx 1, Nqo 1, Prx2 and Prx3 in heart from healthy (AA) and sickle cell (SS)
223 mice under normoxia (N) or exposed to H/R: hypoxia (8% oxygen; 10 hours), followed by reoxy-
224 genation (21% oxygen; 3 hours). 75 μ g/ μ L of protein loaded on an 11% T, 2.5%C polyacrylamide
225 gel. GAPDH serves as protein loading control. One representative gel from 4 with similar results is
226 shown. Densitometric analysis of immunoblots is shown in the right and panels. Data are pre-
227 sented as means \pm SEM (n=4), *p<0.05 compared to normoxia; § p<0.05 compared to AA normoxia
228 by one-way ANOVA.

Figure 8S



229 **Figure 8S. a) Upper panel.** Strategy to identify and hierarchically link target proteins and biological functions and diseases modulated by H/R stress in SS vs AA mice. Experimentally observed

230 target proteins of miRNA modulated in SS vs AA mice, determined by the IPA miRNA target filter

231 analysis, were intersected with modulated proteins identified by proteomic in the same conditions

232 (Figure 2a). Proteins at the intersection were listed in blue and red in the table accordingly to their

233 expression levels as determined by our proteomic characterization. **Lower panel.** Biological pathway

234 Analysis using IPA of merged miRNAs and proteins differentially regulated in SS vs AA mice

235 predicts coherent nodes of miRNA/protein pairs in regulating cardiac hypertrophy, enlargement,

236 and arrhythmia. Differentially expressed miRNA were selected using a fold-change cut-off of 1.5 in

237 4 biological replicates. Differentially expressed proteins were selected using a fold-change cut-off

238 of 1.5 and $p < 0.05$ in $n = 4$ biological replicates. Blue circles: downregulated; red circles: upregulated

239 miRNAs or proteins. **b) Immunoblot analysis,** using specific antibodies against phosphorylated (p-) VEGF receptor (Rec), VEGF Rec, VEGF, Ang1 and Ang2 in heart from healthy (AA) and sickle cell (SS) mice under normoxia (N) and exposed to H/R: hypoxia (8% oxygen; 10 hours), followed by reoxygenation (21% oxygen; 3 hours). 75 $\mu\text{g}/\mu\text{L}$ of protein loaded on an 11% T, 2.5% C polyacrylamide gel. GAPDH serves as protein loading control. One representative gel from 4 with similar results is shown. Densitometric analysis of immunoblots is shown in the right panel. Data are presented as means \pm SEM ($n = 4$), * $p < 0.05$ compared to normoxia; § $p < 0.05$ compared to AA normoxia; ^ $p < 0.05$ compared to AA mice exposed to H/R stress by one-way ANOVA.

240

241

242

243

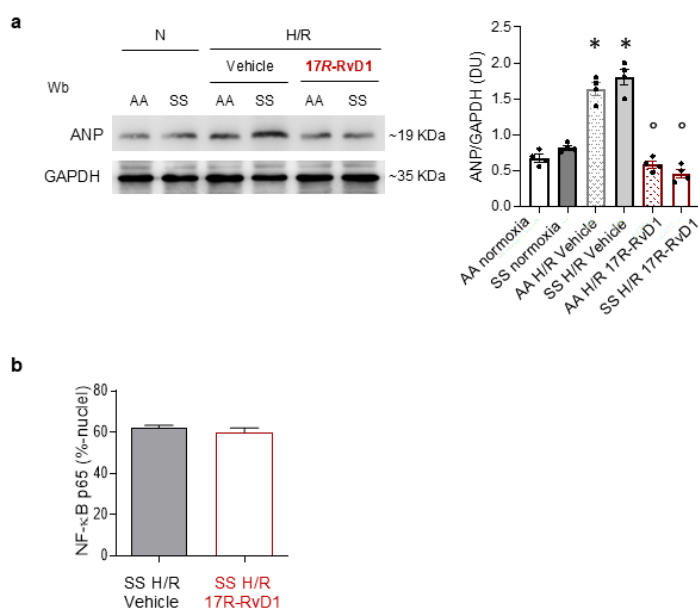
244

245

246

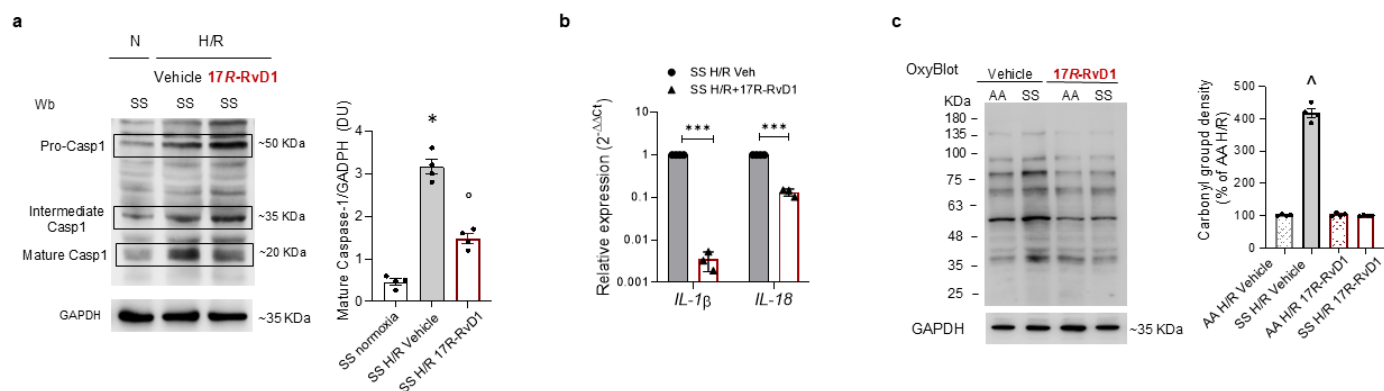
247

Figure 9S



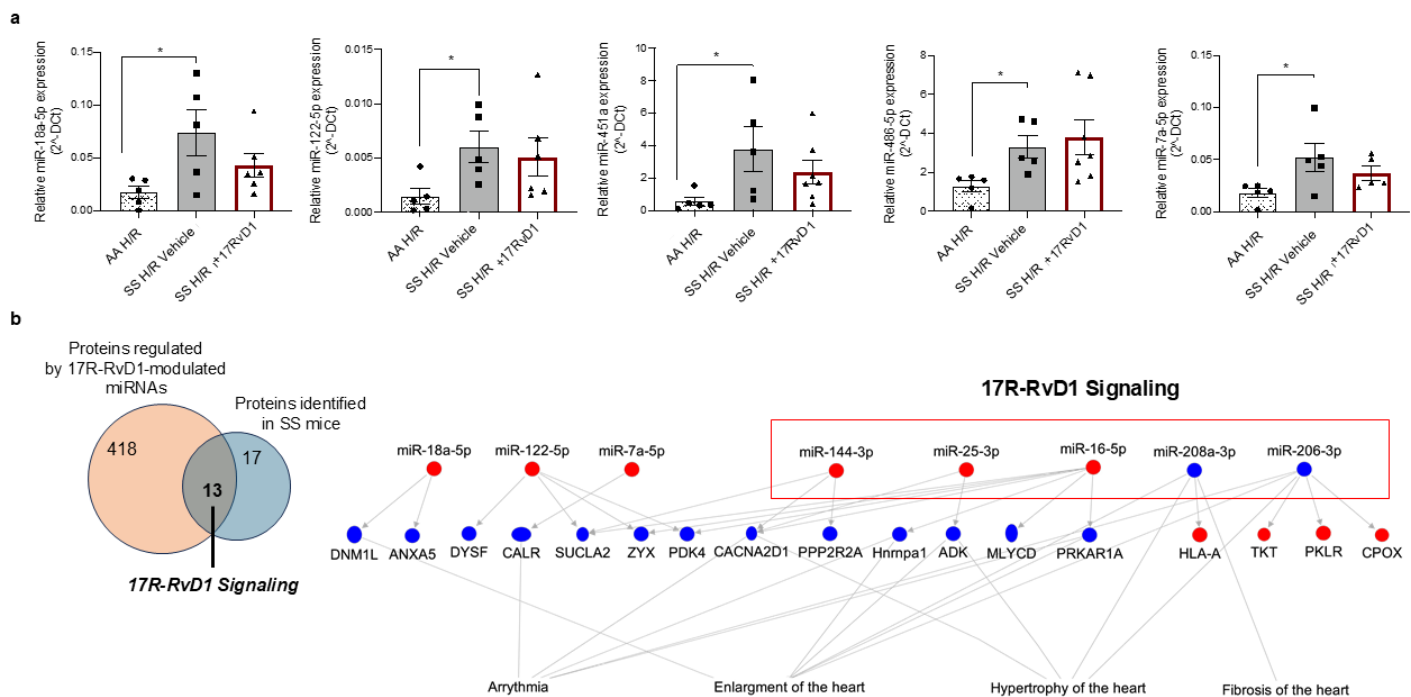
248 **Figure 9S. a)** Immunoblot analysis using specific antibodies against ANP in heart from healthy
 249 (AA) and sickle cell (SS) mice under normoxia and exposed to hypoxia/reoxygenation (H/R) with or
 250 without 17R-RvD1. One representative gel from 4 gels with similar results is shown. Densitometric
 251 analysis of immunoblots is shown in the right panel. Data are presented as means \pm SEM (n=4),
 252 *p<0.05 compared to normoxia; °<0.05 compared to vehicle treated mice by one-way ANOVA. **b)**
 253 Quantification of total NF-κB in heart cells from SS mice undergoing H/R treated with vehicle or 17-
 254 RvD1 from Figure 4a. Results are presented as mean \pm SEM (n=5).

Figure 10S



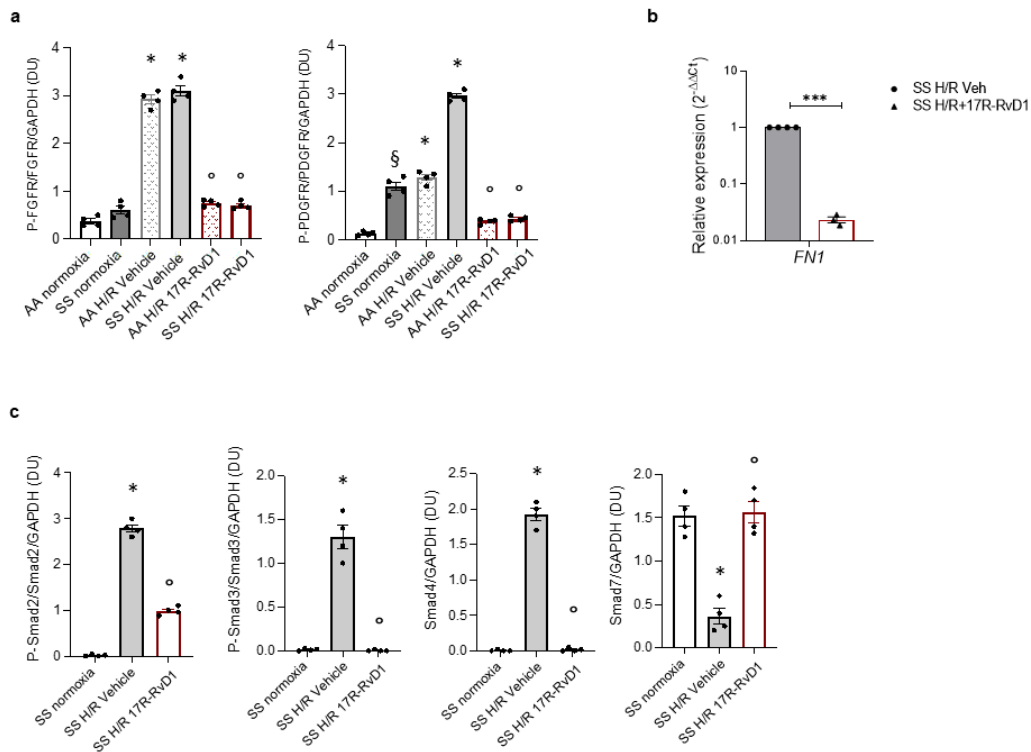
255 **Figure 10S. a)** Immunoblot analysis using specific antibodies against Caspase-1 (Casp-1) in heart
 256 from sickle cell (SS) mice under normoxia and exposed to hypoxia/reoxygenation (H/R) with or
 257 without 17R-RvD1. One representative gel from 4 gels with similar results is shown. Densitometric
 258 analysis of immunoblots is shown in the right panel. Data are presented as means ±SEM (n=4),
 259 *p<0.05 compared to normoxia; °p<0.05 compared to vehicle treated mice by one-way ANOVA. **b)**
 260 RT-PCR analysis of analysis of interleukin 1β (*IL1b*) and interleukin 18 (*IL18*) expression in hearts
 261 from SS mice treated with either vehicle or 17R-RvD1. Data are expressed as fold change com-
 262 pared to SS vehicle. ***p<0.0001 compared to vehicle treated mice Student t-test. **c)** OxyBlot anal-
 263 ysis of the soluble fractions of heart from healthy (AA) and SS mice exposed to H/R: hypoxia (8%
 264 oxygen; 10 hours), followed by reoxygenation (21% oxygen; 3 hours) treated either with vehicle or
 265 17R-RvD1 (100 ng). The carbonylated proteins (1 mg) were detected by treating with 2,4-dinitro-
 266 phenylhydrazine and blotted with anti-DNP antibody. GAPDH serves as protein loading control.
 267 Quantification of band area is shown right panel. Data are presented as means ±SEM (n=4),
 268 ^p<0.05 compared to AA mice exposed to H/R stress; °p<0.05 compared to vehicle treated mice
 269 one-way ANOVA.

Figure 11S



270 **Figure 11S. a)** miRNAs in hearts from SS mice undergoing H/R with or without 17R-RvD1. mi-
271 croRNA expression was determined (using RNU5G and RNU1A1, housekeeping small non-coding
272 RNAs and reported as relative expression levels ($2^{-\Delta Ct}$). *, $p < 0.05$, **, $p < 0.01$ (ANOVA). **b)**
273 Strategy to identify 17R-RvD1 signaling in hearts of SS mice. Experimentally observed target pro-
274 teins of miRNA modulated by 17R-RvD1 in SS mice highlighted with the red box in the hierarchical
275 representation, determined by the IPA miRNA target filter analysis, were intersected with modu-
276 lated proteins identified by proteomic in the same condition. Identified targets modulated key car-
277 diac disease hubs such as arrhythmia, enlargement, hypertrophy, and heart fibrosis.

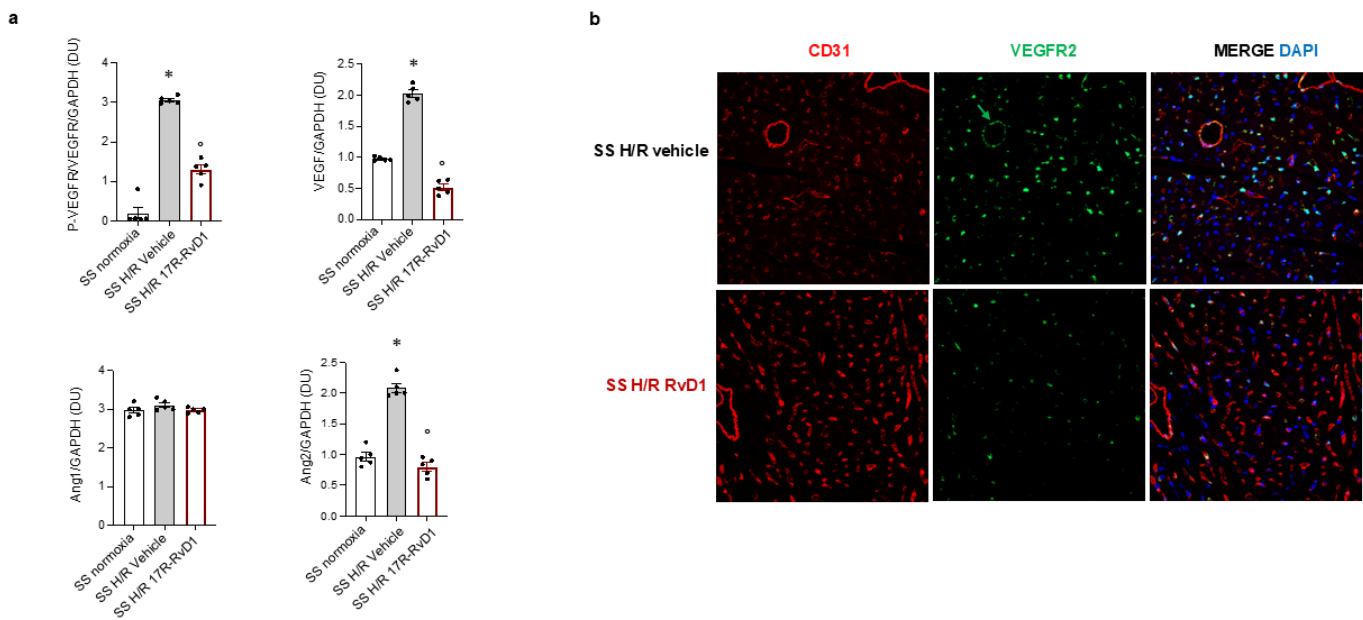
Figure 12S



278 **Figure 12S. a)** Densitometric analysis of immunoblots shown of Figure 6a. Data are presented as
 279 means \pm SEM (n=4), § p<0.05 compared to AA normoxia; *p<0.05 compared to normoxia; °<0.05
 280 compared to vehicle treated mice. **b)** Densitometric analysis of immunoblots shown in Figure 6c.
 281 Data are presented as means \pm SEM (n=4), *p<0.05 compared to normoxia; °p<0.05 compared to
 282 vehicle treated mice one-way ANOVA. **c)** RT-PCR analysis of fibronectin 1 (FN1) expression in
 283 hearts of SS mice treated with vehicle or 17R-RvD1. Data are expressed as fold change compared
 284 to SS vehicle. ***p<0.0001 compared to vehicle treated mice Student t test.

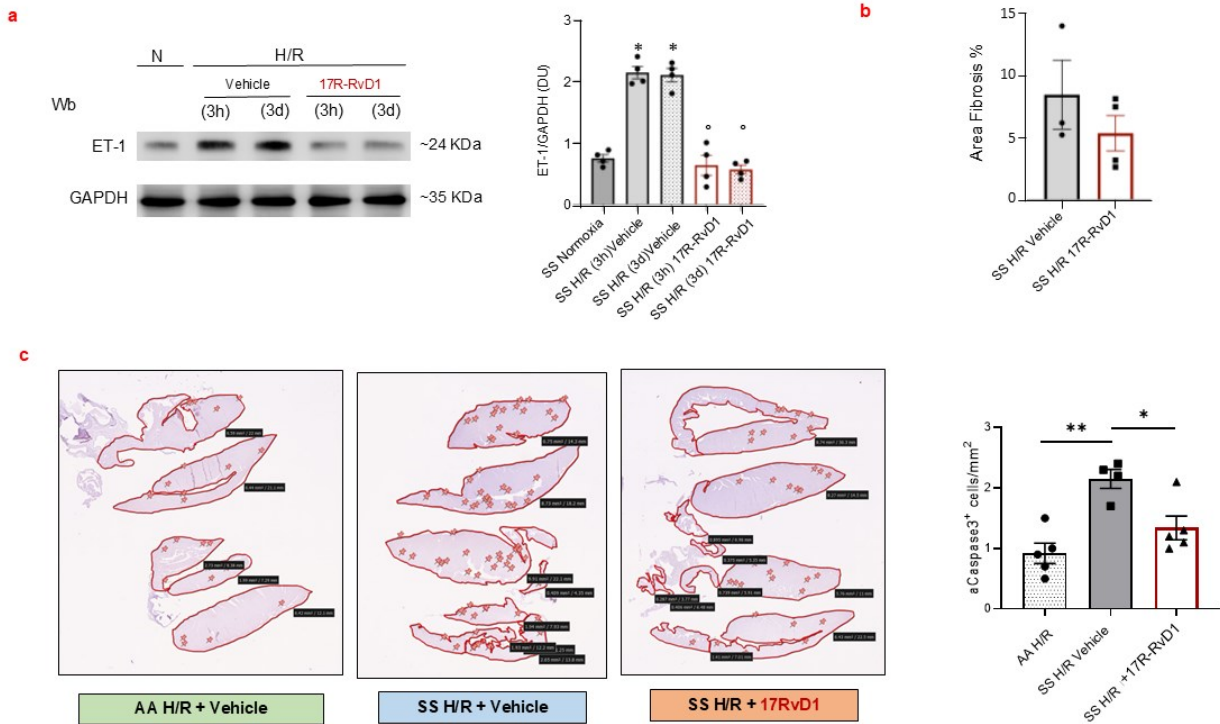
285

Figure 13S



286 **Figure 13S. Left panel.** Densitometric analysis of immunoblots shown in Figure 7b. Data are pre-
287 sented as means \pm SEM (n=5), *p<0.05 compared to normoxia; °<0.05 compared to vehicle treated
288 mice one-way ANOVA. **Right panel.** Individual staining of CD31, VEGFR, and merged images
289 from Figure 6e.

Figure 14S



290 **Figure 14S. a)** Immunoblot analysis using specific antibodies against endothelin-1 (ET-1) in heart
 291 from sickle cell (SS) mice under normoxia and at 3 hours (h) or 3 days (d) after hypoxia/reoxygen-
 292 ation (H/R) stress with or without 17R-RvD1. One representative gel from 4 gels with similar re-
 293 sults is shown. Densitometric analysis of immunoblots is shown in the right panel. Data are pre-
 294 sented as means \pm SEM (n=4), *p<0.05 compared to normoxia; °<0.05 compared to vehicle
 295 treated mice by one-way ANOVA. **b)** Relative quantification in heart sections as Figure 7c from
 296 sickle cell (SS) mice at 3 days after H/R with or without 17-RvD1. Data are presented as means
 297 \pm SEM (n=3-4). **c)** Immunohistochemical staining, and quantification of apoptotic cells (per mm²
 298 heart tissue) identified by labeling for activated caspase-3, in healthy (AA) and sickle (SS) mice
 299 exposed to H/R and treated with vehicle or 17R-RvD1. Data are presented as mean \pm SEM (n =
 300 4-5). *, p < 0.05, **, p < 0.01 (ANOVA).

Table 1S. Echocardiographic parameters of healthy (AA) and sickle cell (SS) mice

	AA	SS	P value
n	8	6	
FS (%)	37.6±2.3	40.0±2.0	0.4684
EF (%)	68.0±3.0	70.5±2.4	0.5397
IVSD (mm)	0.83±0.04	0.92±0.05	0.1629
IVSS (mm)	1.15±0.05	1.31±0.05*	0.0290
LVPWD (mm)	1.04±0.05	1.14±0.07	0.2190
LVPWS (mm)	1.48± 0.08	1.64±0.11	0.2372
LVIDD (mm)	3.70± 0.08	4.50±0.19**	0.0012
LVIDS (mm)	2.31± 0.09	2.69±0.09*	0.0127
LVW (mg)	107.9± 6.7	164.1±18.1*	0.0154
LVEDV (μl)	59.7±3.7	93.7± 9.4**	0.0070
LVESV (μl)	18.1±2.2	27.0±2.1*	0.0138
LVOT CO (ml/min)	22.1±4.3	45.0±12.9	0.0825
LVOT SV (ml)	54.1±5.4	156.8±43.1**	0.0064
MPI	0.62±0.04	0.57±0.07	0.4889
IVRT (ms)	27.6±2.4	18.2±3.8*	0.0349
MVDT (ms)	24.6±2.6	16.7±1.06*	0.0352
MV E/A	1.66±0.14	1.67±0.11	0.9474

NOTE: Mean ± SEM. * $P < 0.05$ and ** $P < 0.01$ by unpaired Student's t test. Abbreviations: FS, fractional shortening; EF, ejection fraction; IVSD, interventricular septal thickness at end-diastole; IVSS, interventricular septal thickness at end-systole; LVPWD, left ventricular posterior wall thickness at end-diastole; LVPWS, left ventricular posterior wall thickness at end-systole; LVEDD, left ventricular end-diastolic diameter; LVEDS, left ventricular end-systolic diameter; LVM, left ventricle mass; LVEDV, left ventricle end-diastolic volume; LVESV, left ventricle end-systolic volume; LVOT CO, left ventricle outflow tract cardiac output; LVOT SV, left ventricle outflow tract stroke volume; IVRT, isovolumetric relaxation time; MPI, myocardial performance index; MVDT, mitral valve deceleration time; MV E/A, mitral valve E/A.

308
309

Table 2S. Echocardiographic parameters pre- and post-H/R of SS mice treated with either 17R-RvD1 or vehicle

	SS vehicle		SS 17R-RvD1		
	pre-H/R	post-H/R	pre-H/R	post-H/R	P value
n	3	3	4	4	
FS (%)	38.5±2.7	32.1±0.8	41.0±1.8	40.2±2.8*	0.0328
EF (%)	69.0±3.5	60.4±1.1	72.2±2.4	71.0±3.6*	0.0313
LVAWD (mm)	0.93±0.09	0.91± 0.10	0.77± 0.06	0.79± 0.06	0.2756
LVAWS (mm)	1.39± 0.05	1.45± 0.09	1.41± 0.08	1.40± 0.09	0.6875
LVPWD (mm)	0.86±0.03	0.89±0.03	0.87±0.06	1.02±0.12	0.2884
LVPWS (mm)	1.31±0.06	1.21±0.09	1.20±0.09	1.37±0.15	0.3458
LVIDD (mm)	4.23±0.28	4.48±0.19	4.11±0.33	4.11±0.33	0.4080
LVIDS (mm)	2.61±0.28	3.04±0.12	2.44±0.26	2.48±0.31	0.1763
LVW (mg)	121.8±17.9	132.8±2.3	104.8±20.8	116.5±13.0	0.4967
LVEDV (μl)	80.8±12.4	92.2±8.8	76.9±14.6	76.7±14.8	0.4491
LVESV (μl)	25.9±6.4	36.4±3.3	22.2±6.3	23.8±7.2	0.1935
LVOT CO (ml/min)	17.8±1.5	18.7±2.0	15.9±1.5	16.4±2.1	0.3942
LVOT SV (ml)	55.0±6.1	55.7±5.8	54.6±8.6	52.9±7.6	0.8015
MPI	0.55±0.05	0.55±0.08	0.60±0.06	0.53±0.03	0.8355
IVRT (ms)	29.3±3.7	24.1±2.0	32.3±6.6	27.1±2.0	0.6421
MVDT (ms)	19.0±4.1	21.2±1.0	21.3±3.6	28.8±2.8	0.1274
MV E/A	1.64±0.13	1.87±0.13	1.53±0.14	1.45±0.15	0.0631

310 NOTE: Mean ± SEM. P values refer to vehicle post-H/R versus SS 17R-RvD1 post-H/R; *P<0.05 SS vehicle post-H/R versus SS 17R-
311 RvD1 post-H/R by two-way repeated measures ANOVA followed by Fishier LSD post hoc test.

312 Abbreviations: FS, fractional shortening; EF, ejection fraction; LVAWD, left ventricular anterior wall thickness at end-diastole; LVAWS, left
313 ventricular anterior wall thickness at end-systole; LVPWD, left ventricular posterior wall thickness at end-diastole; LVPWS, left ventricular
314 posterior wall thickness at end-systole; LVEDD, left ventricular end-diastolic diameter; LVEDS, left ventricular end-systolic diameter; LVM,
315 left ventricle mass; LVEDV, left ventricle end-diastolic volume; LVESV, left ventricle end-systolic volume; LVOT CO, left ventricle outflow
316 tract cardiac output; LVOT SV, left ventricle outflow tract stroke volume; IVRT, isovolumetric relaxation time; MPI, myocardial performance
317 index; MVDT, mitral valve deceleration time; MV E/A, mitral valve E/A.

Figure 1c

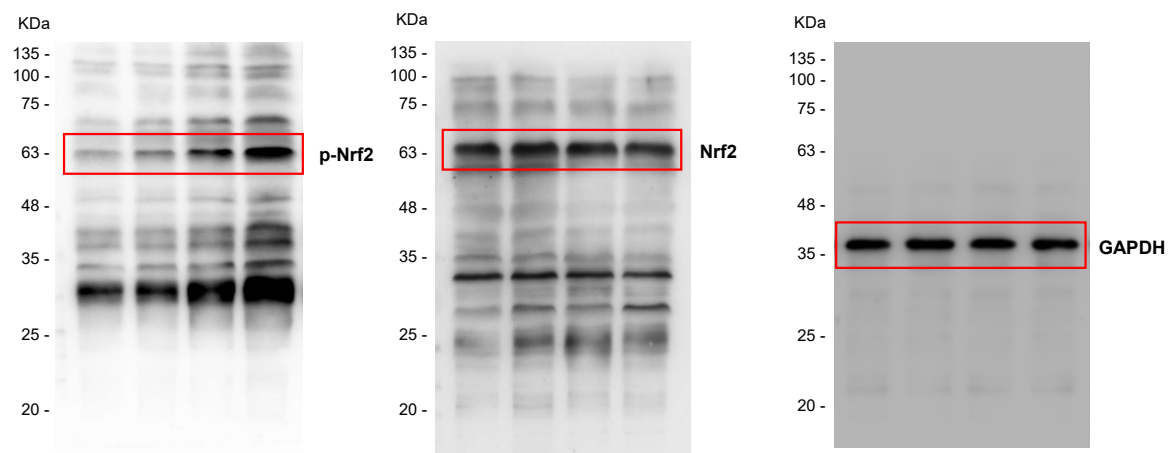


Figure 1d

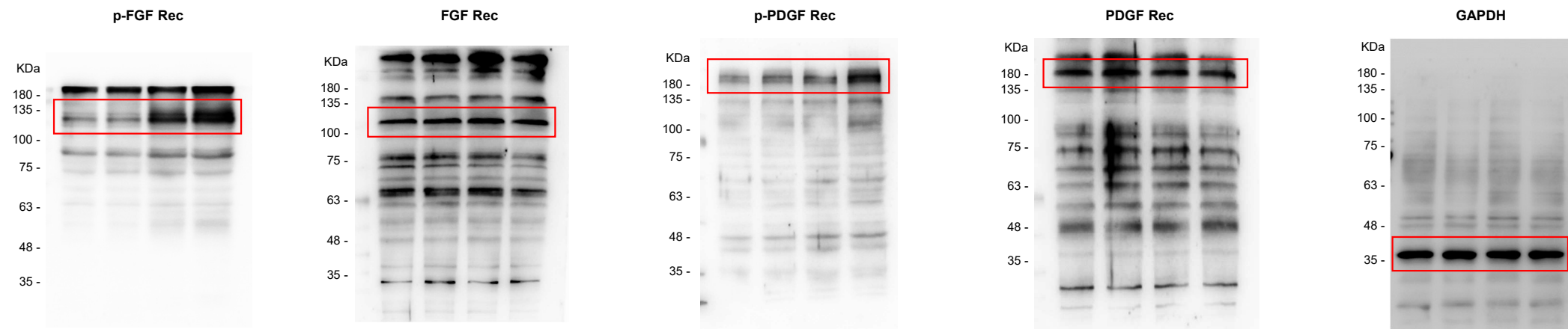


Figure 1e

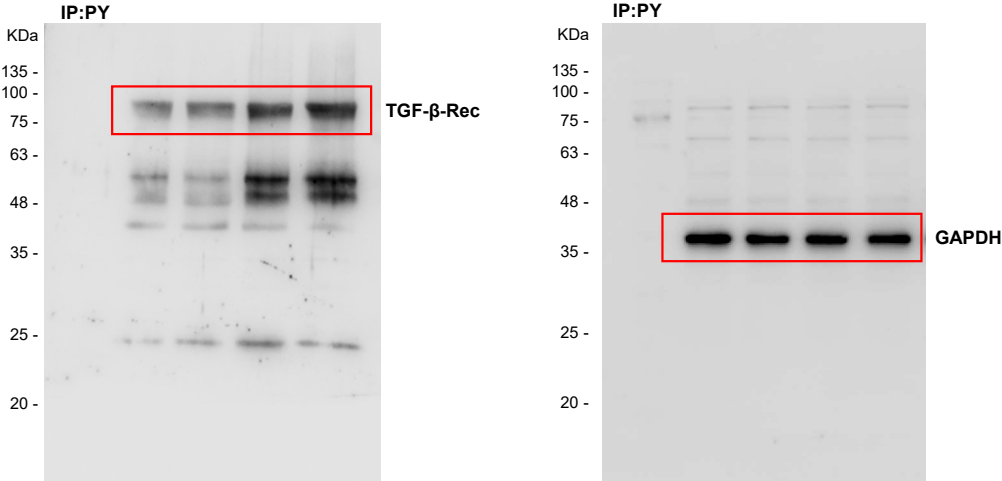


Figure 4a

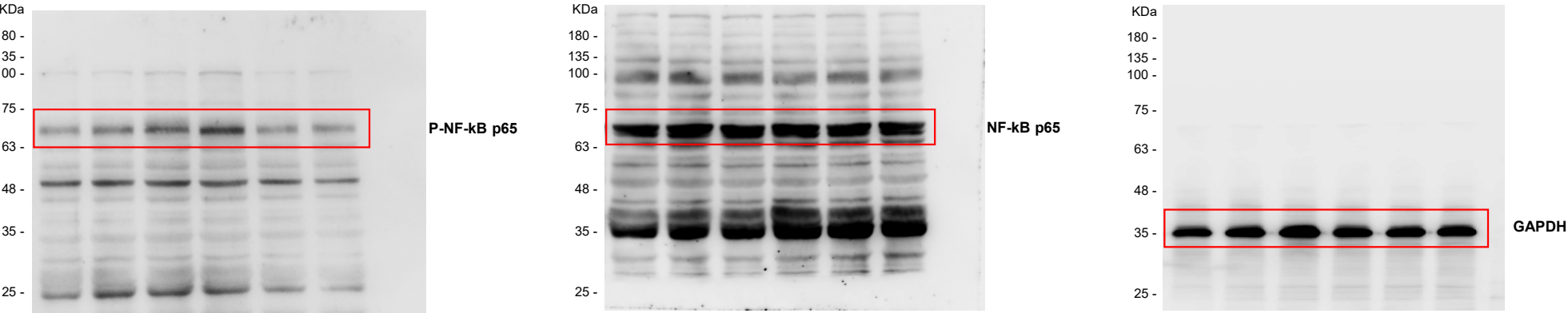


Figure 4b

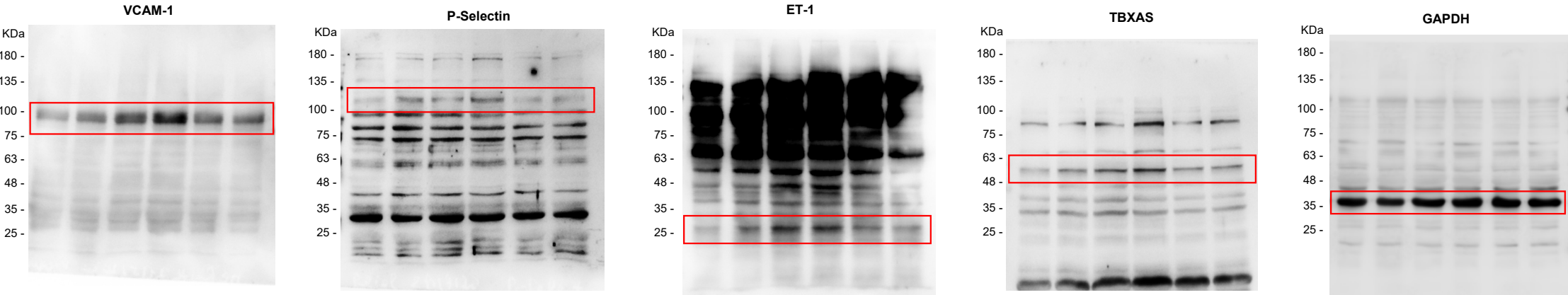


Figure 4c

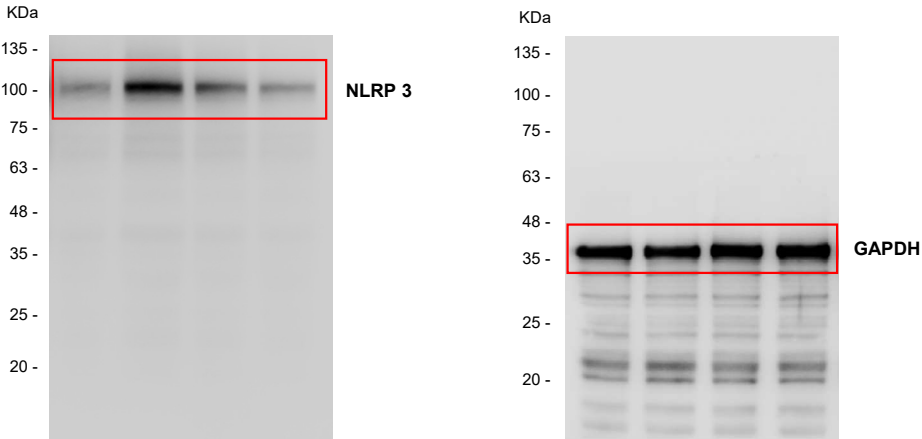


Figure 5a

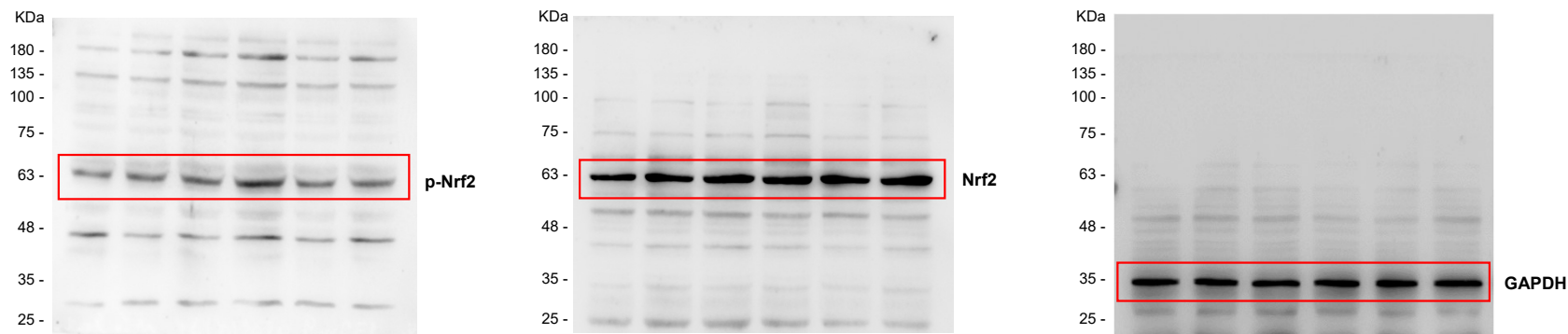


Figure 5b

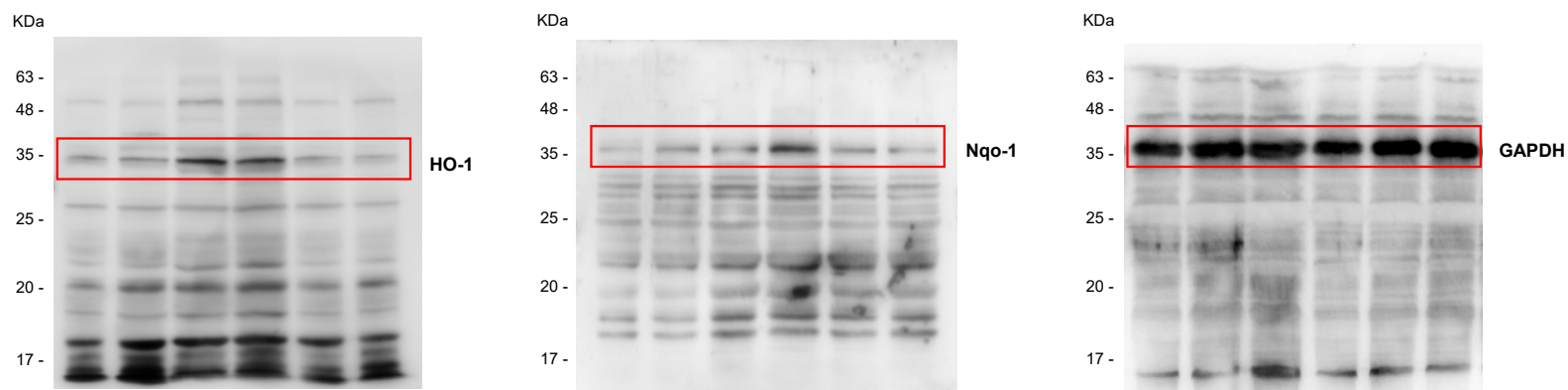


Figure 5c

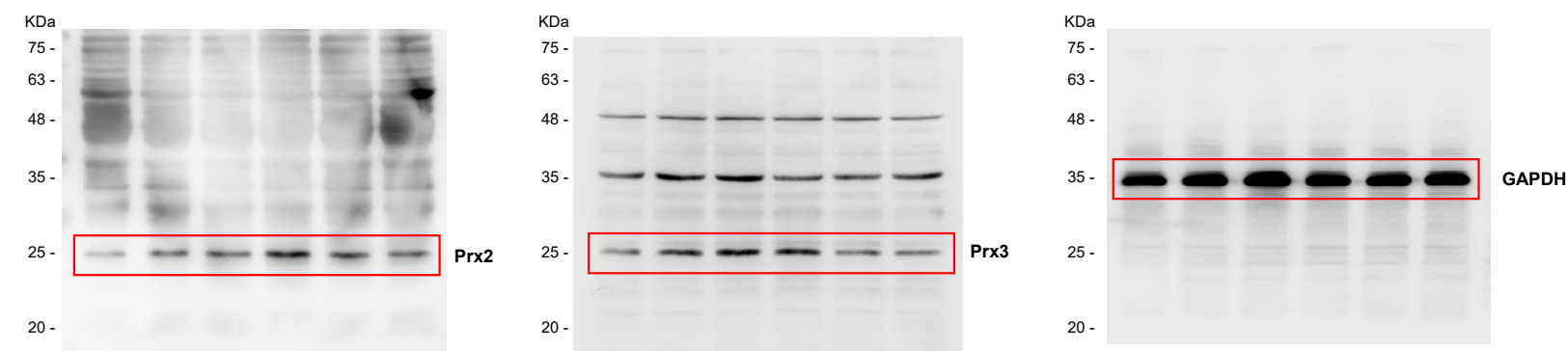


Figure 6a

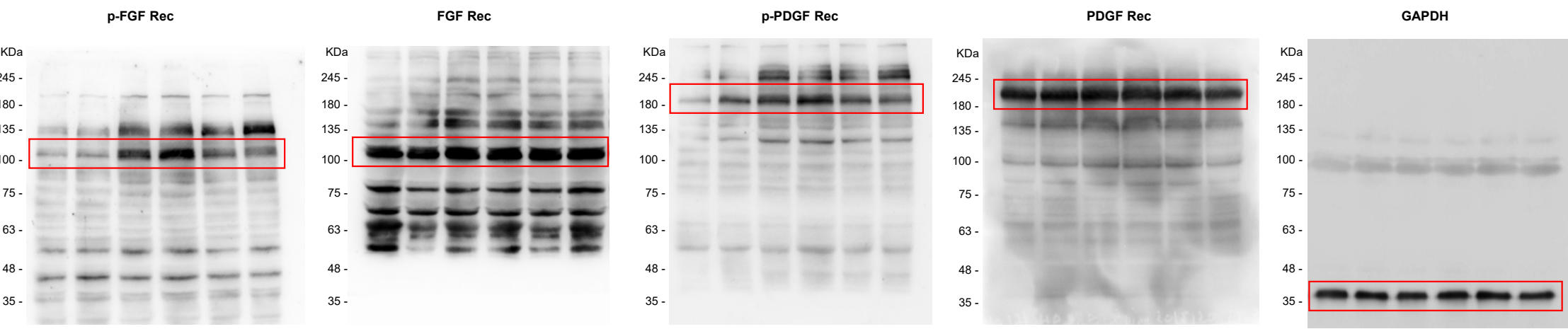


Figure 6b

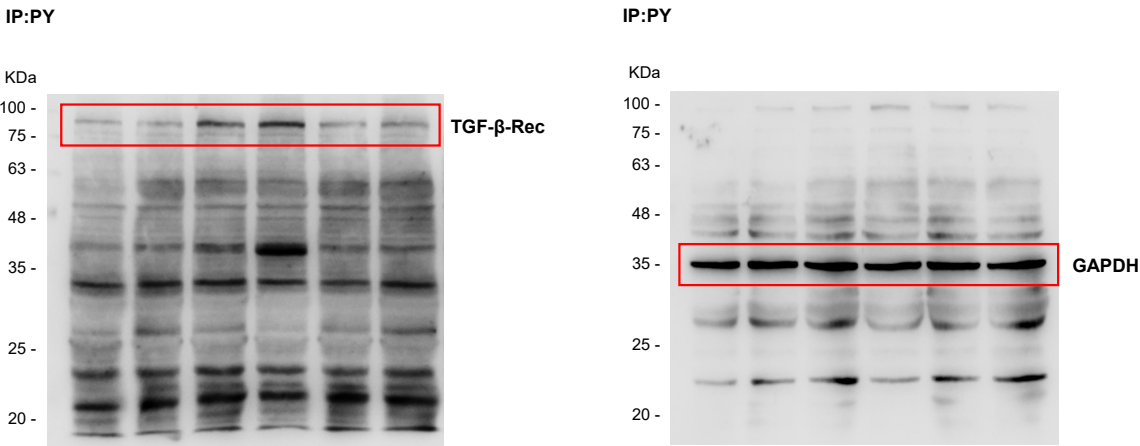


Figure 6c

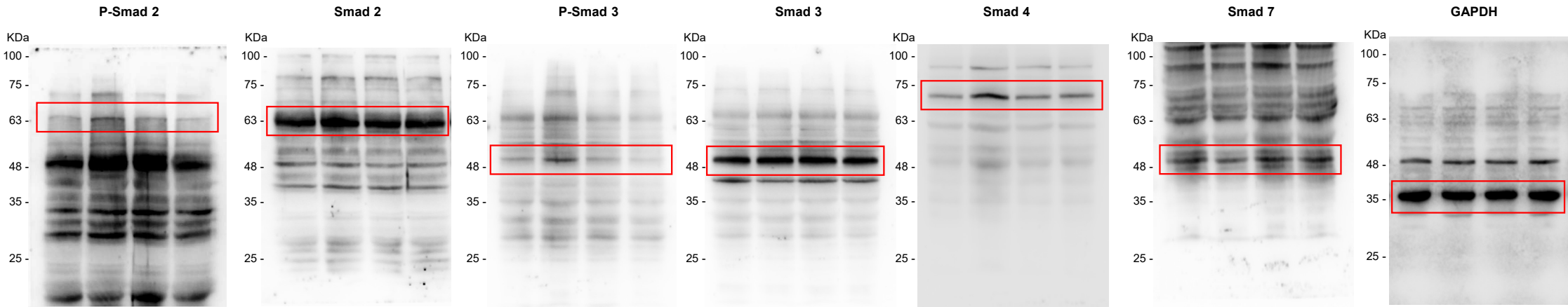


Figure 6d

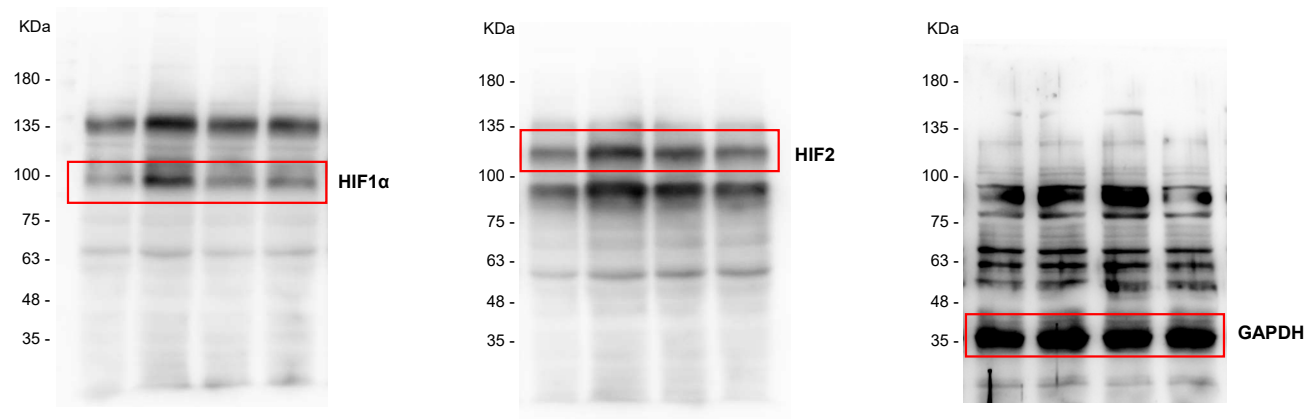


Figure 6e

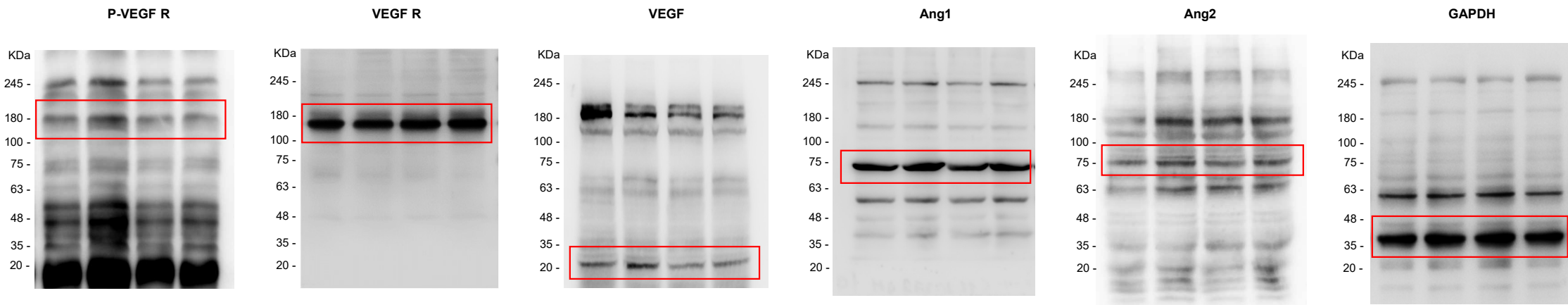


Figure 7d

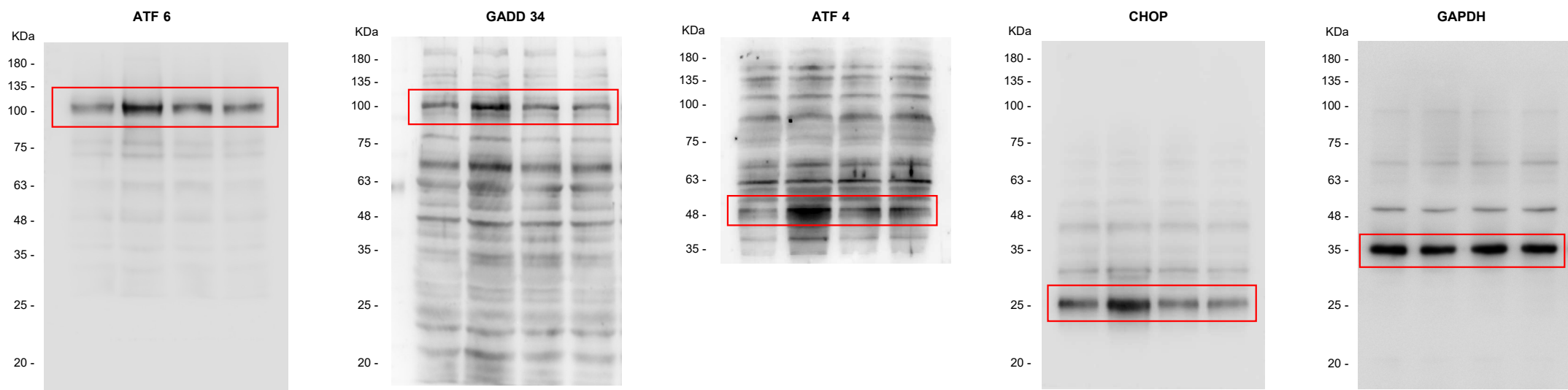


Figure 7e

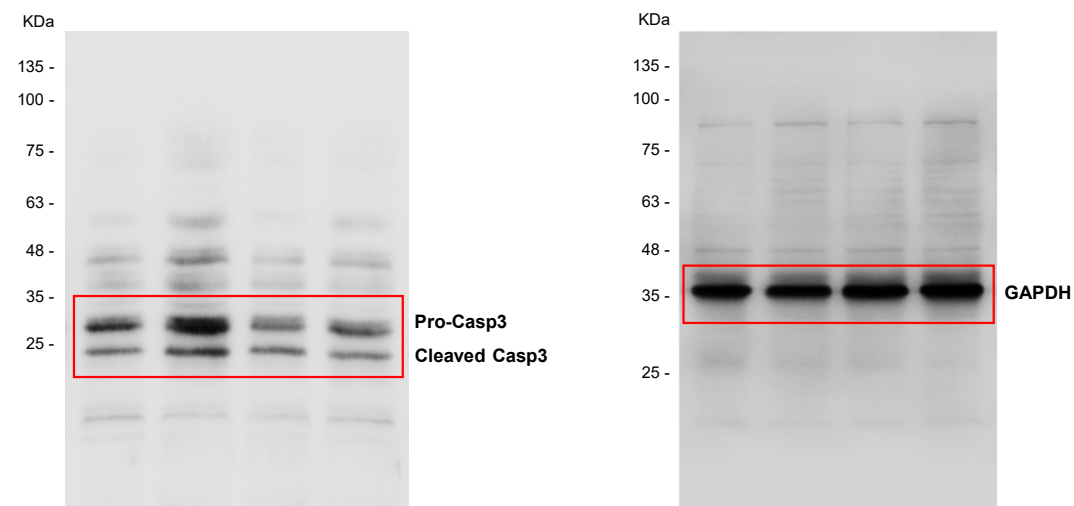


Figure 2Sa

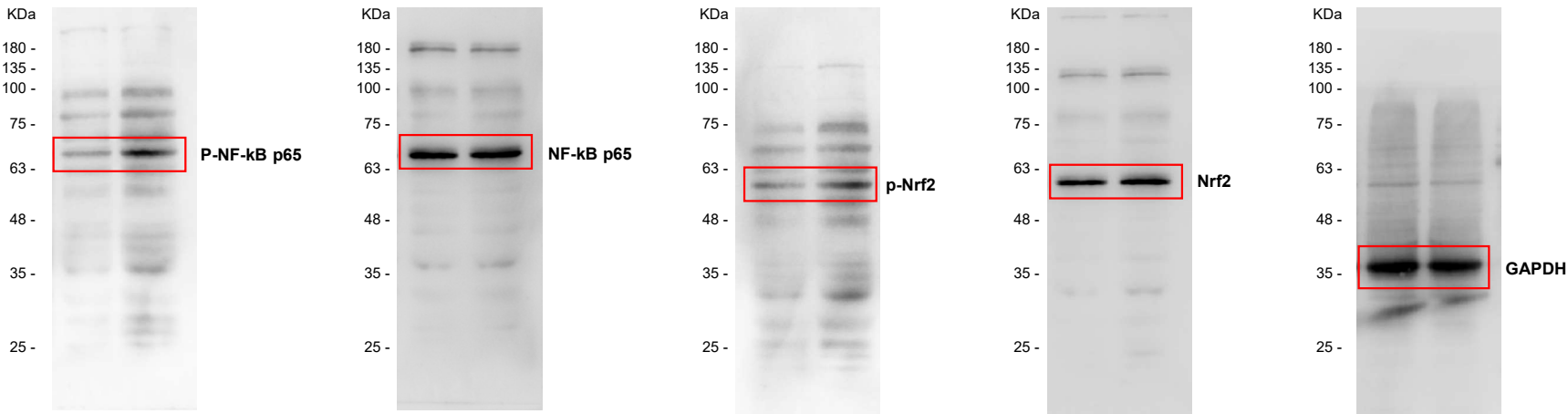


Figure 2Sb

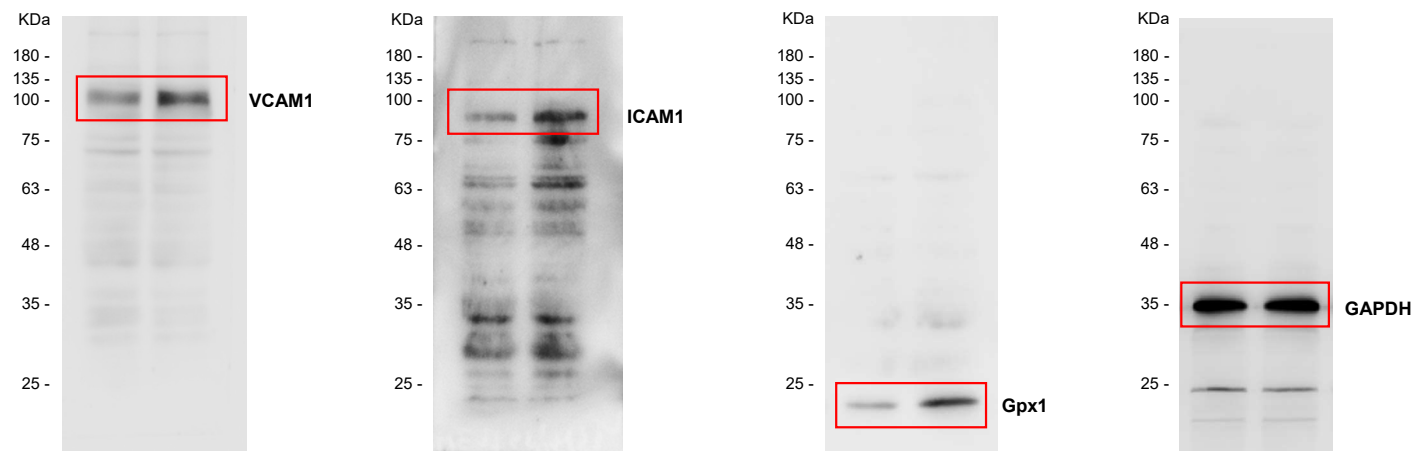


Figure 3Sc

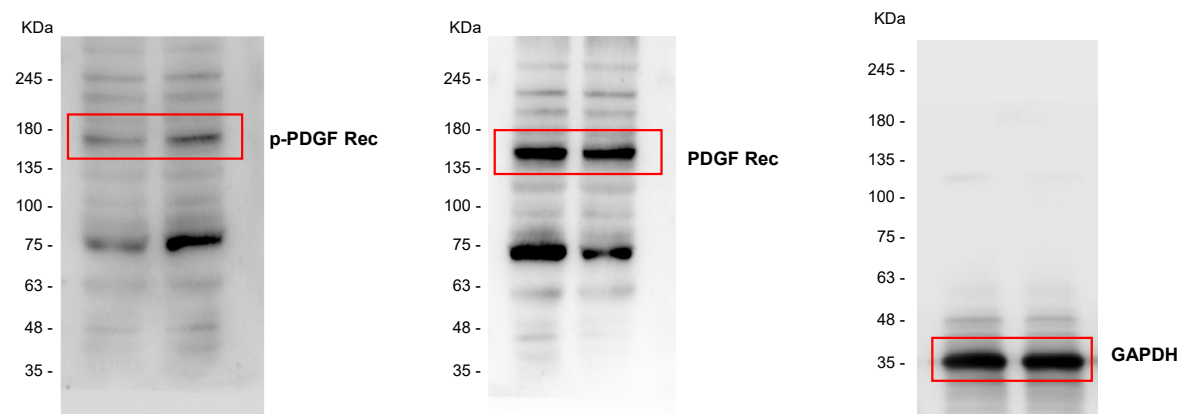


Figure 6Sa

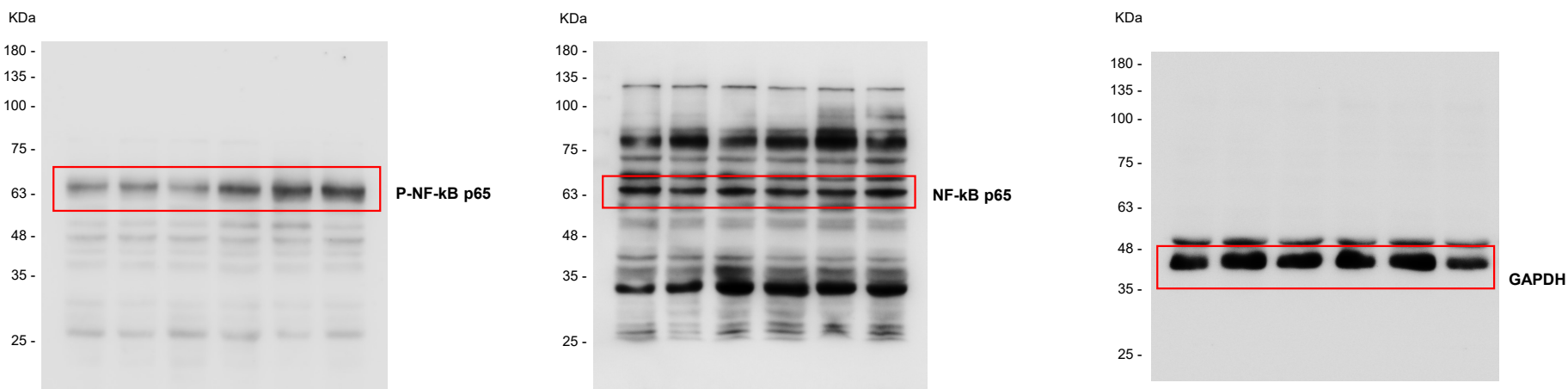


Figure 6Sb

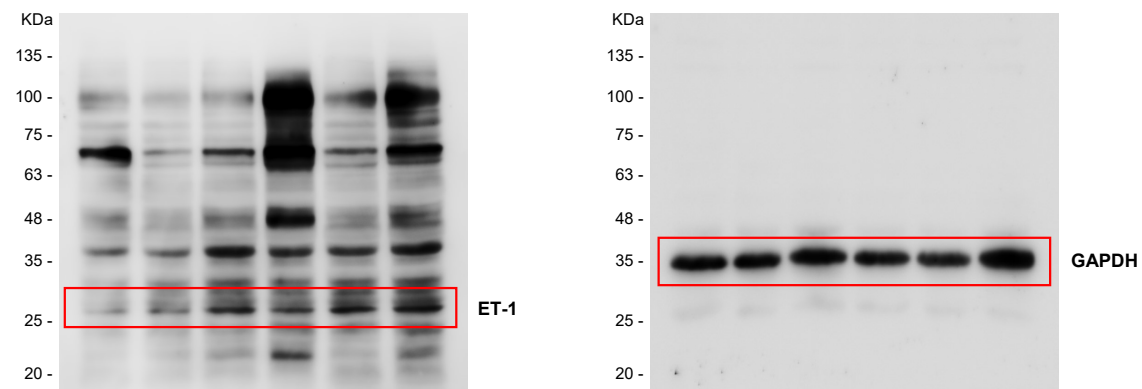


Figure 6Sc

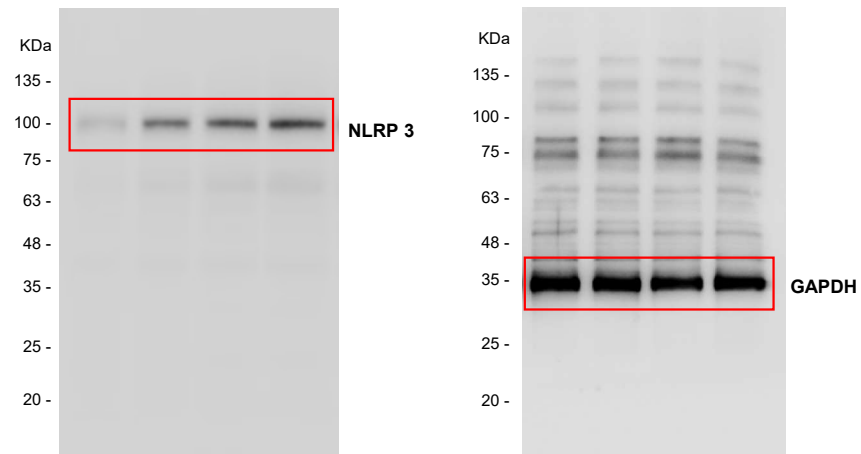


Figure 7Sa

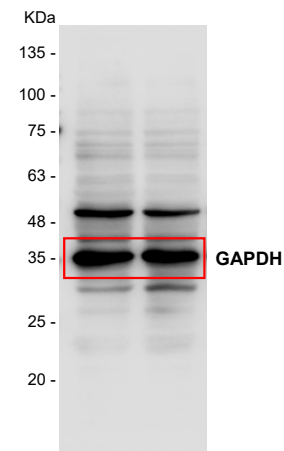


Figure 7Sb

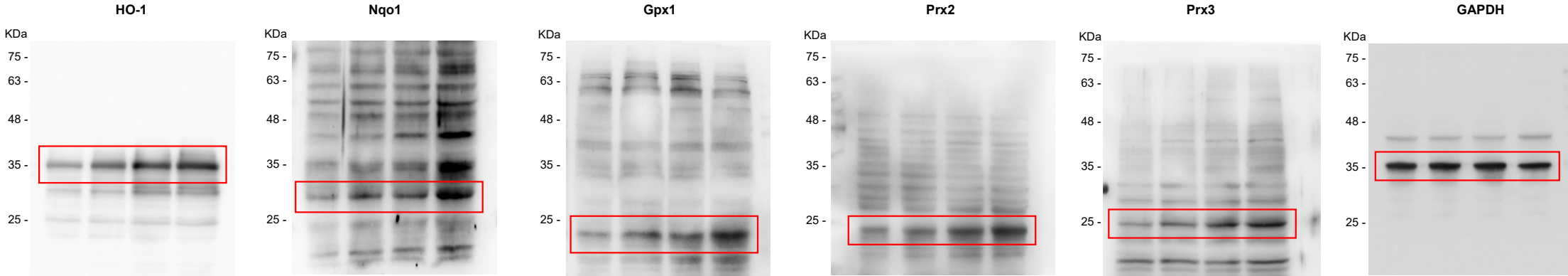


Figure 8Sb

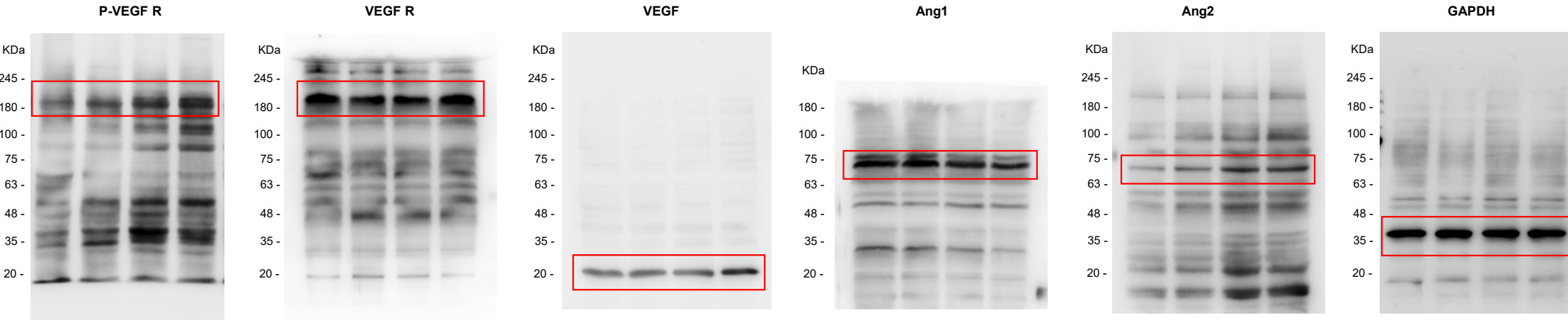


Figure 9Sa

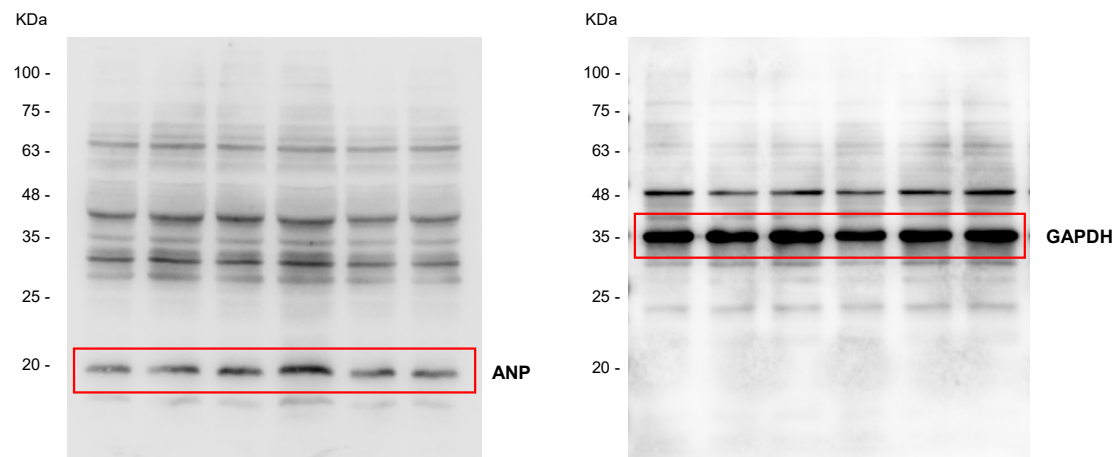


Figure 10Sa

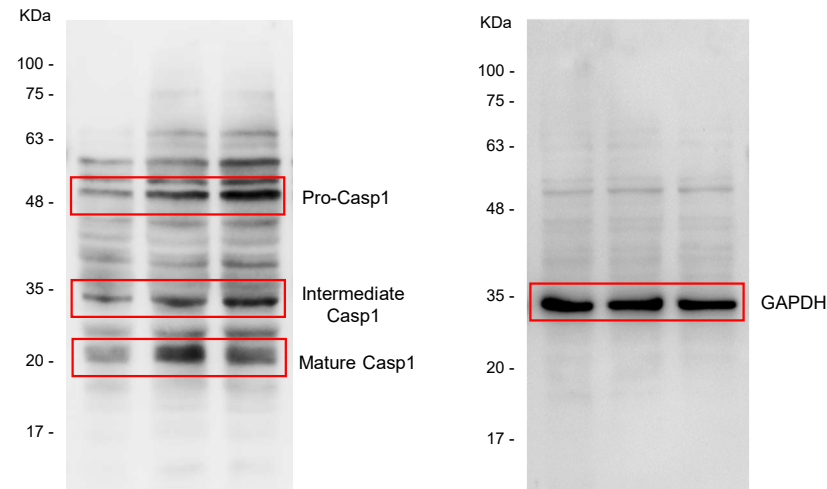


Figure 10Sc

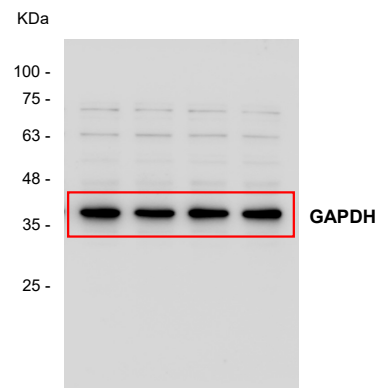


Figure 14Sa

